A Model for the Photosystem II Reaction Center Core Including the Structure of the Primary Donor P_{680}[†,‡]

Bengt Svensson,[§] Catherine Etchebest,[∥] Pierre Tuffery,[⊥] Paul van Kan,[§,#] Jeremy Smith,[○] and Stenbjörn Styring*[,§,#]

Department of Biochemistry, Arrhenius Laboratories for Natural Sciences, Stockholm University, S-106 91 Stockholm, Sweden, Biochemistry, Center for Chemistry and Chemical Engineering, Lund University, P.O. Box 124, S-221 00 Lund, Sweden, Laboratoire de Biochimie Théorique, Institut de Biologie Physico-Chimique, 13 rue Pierre et Marie Curie, 75005 Paris, France, URBB, U263 INSERM, Universite Paris 7, 2 Place Jussieu, 75251 Paris Cedex 05, France, and Section de Biophysique des Protéines et des Membranes, Département de Biologie Cellulaire et Moléculaire, Centre d'Etudes Saclay, 91191 Gif-sur-Yvette Cedex, France

Received April 1, 1996; Revised Manuscript Received August 26, 1996[⊗]

ABSTRACT: For a detailed understanding of the function of photosystem II (PSII), a molecular structure is needed. The crystal structure has not yet been determined, but the PSII reaction center proteins D1 and D2 show homology with the L and M subunits of the photosynthetic reaction center from purple bacteria. We have modeled important parts of the D1 and D2 proteins on the basis of the crystallographic structure of the reaction center from *Rhodopseudomonas viridis*. The model contains the central core of the PSII reaction center, including the protein regions for the transmembrane helices B, C, D, and E and loops B−C and C−D connecting the helices. In the model, four chlorophylls, two pheophytins, and the nonheme Fe^{2+} ion are included. We have applied techniques from computational chemistry that incorporate statistical data on side-chain rotameric states from known protein structures and that describe interactions within the model using an empirical potential energy function. The conformation of chlorophyll pigments in the model was optimized by using exciton interaction calculations in combination with potential energy calculations to find a solution that agrees with experimentally determined exciton interaction energies. The model is analyzed and compared with experimental results for the regions of P_{680}, the redox active pheophytin, the acceptor side Fe^{2+}, and the tyrosyl radicals Tyr_D and Tyr_Z. P_{680} is proposed to be a weakly coupled chlorophyll *a* pair which makes three hydrogen bonds with residues on the D1 and D2 proteins. In the model the redox-active pheophytin is hydrogen bonded to D1-Glu130 and possibly also to D1-Tyr126 and D1-Tyr147. Tyr_D is hydrogen bonded to D2-His190 and also interacts with D2-Gln165. Tyr_Z is bound in a hydrophilic environment which is partially constituted by D1-Gln165, D1-Asp170, D1-Glu189, and D1-His190. These polar residues are most likely involved in proton transfer from oxidized Tyr_Z or in metal binding.

In oxygenic photosynthesis in plants, algae, and cyanobacteria, photosystem II (PSII)[1] carries out the light-driven reduction of plastoquinone by electrons derived from water. The PSII complex is composed of more than 20 polypeptide subunits (Andersson & Styring, 1991; Vermaas et al., 1993). It is widely accepted that the integral membrane proteins D1 and D2 constitute the PSII reaction center and form a heterodimer that binds the redox components necessary for the primary electron transfer reactions (Nanba & Satoh, 1987). These bound redox components include the primary electron donor, P_{680}, the acceptor complex including the intermediary pheophytin acceptor, the first and second quinone acceptors, Q_A and Q_B, and the Fe^{2+} ion. On the donor side, the heterodimer contains two redox-active tyrosine residues: the immediate electron donor to P_{680}^+, Tyr_Z on the D1 protein (Debus et al., 1988a; Metz et al., 1989), and an accessory electron donor, Tyr_D on the D2 protein (Debus et al., 1988b; Vermaas et al., 1988). The D1/D2 heterodimer probably also binds the Mn cluster involved in the water oxidation reaction, which consists of four Mn ions, and also binds a Ca^{2+} ion (Debus, 1992).

The three-dimensional structure of the PSII reaction center has not yet been determined. However, the D1 and D2

† This work was supported by the Swedish Natural Science Research Council and the Carl Trygger Foundation. B.S. gratefully acknowledges fellowships from the ESF programme on Biophysics in Photosynthesis, C. F. Liljewalchs, Jr.'s, Resestipendier, and Wallenberg Stiftelsens Jubileums fond. P.v.K. acknowledges fellowships from the NWO and the EMBO.

‡ The coordinates for the structural model of PSII, as presented in this publication, have been deposited at the Brookhaven Protein Data Bank under the filename 1DOP.

* Author to whom correspondence should be addressed at Lund University.

§ Stockholm University.

∥ Institut de Biologie Physico-Chimique.

⊥ Universite Paris 7.

Lund University.

○ Centre d'Etudes Saclay.

⊗ Abstract published in *Advance ACS Abstracts,* October 15, 1996.

[1] Abbreviations: $Chl_{D1,P680}$ and $Chl_{D2,P680}$, the chlorophylls of P_{680} associated with the D1 and D2 proteins, respectively; $Chl_{D1,acc}$ and $Chl_{D2,acc}$, the accessory chlorophylls associated with the D1 and D2 proteins, respectively; CP43 and CP47, the chlorophyll binding inner antenna proteins of the photosystem II complex; D1 and D2, polypeptides of the photosystem II reaction center; *C. reinhardtii, Chlamydomonas reinhardtii*; ENDOR, electron nuclear double resonance; EPR, electron paramagnetic resonance; ESEEM, electron spin-echo envelope modulation; P_{680}, the primary electron donor of photosystem II; PSII, photosystem II; Q_A and Q_B, the primary and secondary quinone acceptors; *Rb. capsulatus*, *Rhodobacter capsulatus*; *Rb. sphaeroides*, *Rhodobacter sphaeroides*; *Rps. viridis*, *Rhodopseudomonas viridis*; Tyr_D, the accessory tyrosyl radical in photosystem II, D2-Tyr161; Tyr_Z, the redox-active tyrosyl radical in photosystem II, D1-Tyr161.

S0006-2960(96)00764-7 CCC: $12.00

proteins show a sequence identity of approximately 20% with their equivalents from purple bacteria, the L and M subunits (Williams et al., 1983, 1984; Youvan et al., 1984; Michel et al., 1986). This sequence homology places PSII in the "gray zone" for sequence homology modeling; *i.e.*, one cannot be sure *per se* that the backbone fold of PSII will follow that of the bacterial reaction centers. However, additional evidence exists suggesting that structural homology should exist. Antibody binding studies showed that each of the D1 and D2 proteins spans the membrane five times, as in the purple bacteria (Sayre et al., 1986). There are also functional analogies between PSII and the purple bacterial reaction centers. These involve especially the pheophytin acceptor and the secondary charge stabilization reactions involving electron transfer from the pheophytin to Q_A and to Q_B (Wraight, 1982). The cofactors involved in these steps are chemically related, and spectroscopic results concerning the intermediate acceptor pheophytin (Lubitz et al., 1989; Moënne-Loccoz et al., 1989; Nabedryk et al., 1990) and Q_A and Q_B (Rutherford, 1987) indicate that these components are probably bound in a similar fashion in the two systems. Furthermore, the fact that the herbicide azidoatrazine binds to both the D1 protein and the L subunit (Pfister et al., 1981; De Vitry & Diner, 1984) also suggests that there are structural similarities in the Q_B site. The resemblance is also substantiated by the identification of point mutations in homologous positions in the D1 protein and the L that give rise to resistance against herbicides binding in the Q_B niche (Trebst, 1986).

The available evidence suggests that the use of the purple bacterial reaction center as template for PSII homology modeling may provide useful information in determining the structure of cofactor binding sites in PSII. This has allowed assignment of functionally and/or structurally important residues (Michel et al., 1986; Trebst, 1986; Michel & Deisenhofer, 1988; Svensson et al., 1990; Otsuka et al., 1992; Ruffle et al., 1992). Several models derived by exploiting the homology exist for various regions of PSII. By exchanging a small number of side chains in the *Rhodopseudomonas viridis* structure (Deisenhofer et al., 1985) to the corresponding PSII residues, we graphically modeled Tyr_Z and Tyr_D on the donor side of PSII (Svensson et al., 1990, 1991). Several aspects of the model have been confirmed by a combination of site-directed mutagenesis and spectroscopy (Tommos et al., 1993, 1994; Tang et al., 1993; Roffey et al., 1994b). Attempts have also been made to model the herbicide-binding niche in the Q_B site of the D1 protein (Trebst, 1987; Crofts et al., 1987; Bowyer et al., 1990; Tietjen et al., 1991; Ohad et al., 1992; Egner et al., 1993, Sobolev & Edelman, 1995). "Knowledge"-based homology modeling techniques, involving data-bank searches for loop structures, have also been used to model the entire D1/D2 heterodimer (Ruffle et al., 1992).

In this paper we present a model for the core of the PSII reaction center of spinach and the associated cofactors based on homology considerations and energy calculations. The aim has been to create a structural model which accommodates all relevant experimental results. First, the backbone was transferred where possible from the *Rps. viridis* template structure to PSII. Second, the side chains were positioned and small backbone adjustments made using methods that combine statistical data of side-chain orientations (Tuffery et al., 1991) with a description of physical interactions using a molecular mechanics energy function (Brooks et al., 1983). The model also includes a proposal for the structure of the primary donor, P_{680}, which is correlated with known data on P_{680} obtained with optical spectroscopy. The model allows the interpretation of experimental data on the cofactor binding sites and is used to suggest further experiments with the aim of improving the model and further elucidating the role of specific residues in PSII function.

METHODS AND DATA

The modeling procedure described below comprises a combination of computational approaches and is as follows: determination of regions that are likely to be structurally conserved; transfer of atomic coordinates, including PSII cofactors; positioning of nonconserved amino acid side chains using a rotamer library; minimization of the potential energy; optimization of side-chain and pigment interactions using energy calculations; evaluation of the structural quality; and, finally, comparison with experimental data.

Homology Modeling. The present modeling was made only of those regions with highest homology with the template protein, the photosynthetic reaction center from *Rps. viridis* (Deisenhofer et al., 1985; Deisenhofer & Michel, 1989). The model consists of the most central parts of the D1 and D2 proteins and the cofactors bound in these regions (Figure 1). It contains eight transmembrane helices, 302 amino acids, a chlorophyll dimer, two monomeric chlorophylls, two pheophytins, and a Fe^{2+} ion (Svensson et al., 1992). There is 22% sequence identity (66 identical residues) between PSII and *Rps. viridis* in this region (Michel & Deisenhofer, 1988). The regions excluded from the modeling are the N-terminus, the first transmembrane helix, the A−B loop, the D−E loop, and the C-terminus. These regions are more difficult to treat as they are less homologous with *Rps. viridis* and also because they vary significantly between D1 and D2 proteins of different species (Svensson et al., 1991) and tend to be external and in contact with other subunits.

The 2.3 Å resolution structure of the photosynthetic reaction center from *Rps. viridis* (Deisenhofer et al., 1985; Deisenhofer & Michel, 1989) was used, *i.e.*, the 1PRC entry in the Brookhaven Protein Data Bank (Bernstein et al., 1977). Atomic coordinates for the backbone and the identical side chains were directly transferred to the PSII model. Coordinates for the four bacteriochlorophyll *b* and two bacteriopheophytin *b* molecules were transferred for those atoms which are chemically identical in chlorophyll *a* and pheophytin *a*. The nonidentical atoms in the chromophores were inserted with standard geometry with the program CHARMM (Brooks et al., 1983).

Initial Side-Chain Orientation. The side chains of identical residues in homologous proteins have a high probability of adopting the same conformation (Summers et al., 1987). Therefore, the coordinates of all identical residues were fixed. To position the nonidentical side chains, the sparse-matrix-driven (SMD) algorithm was used (Tuffery et al., 1991). This is based on a rotamer library obtained from an analysis of torsion angles present in structures determined to high resolution. The PSII cofactors (a chlorophyll dimer, two monomeric chlorophylls, two pheophytins, and a Fe^{2+} ion) were at this stage in the calculations fixed.

Molecular Mechanics Calculations. The SMD-derived PSII model was used as an input for molecular mechanics

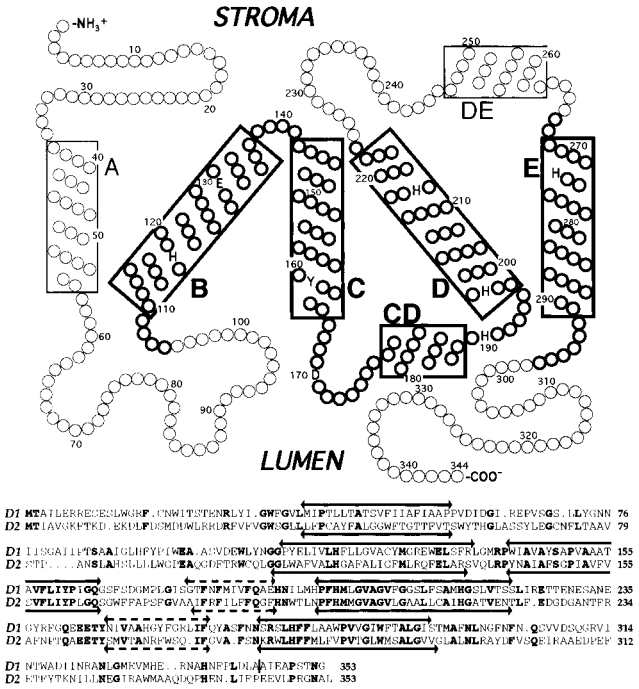

FIGURE 1: Predicted folding pattern for the D1 protein (the D2 protein is almost identical). The transmembrane helices B, C, D, and E and the loop connecting the C and D helices are drawn in bold. These are the regions of both the D1 and D2 proteins, which are included in our calculations. Amino acids with a proposed function are shown with their one-letter code: D1-His118, possible chlorophyll ligand; D1-Glu130, hydrogen bonding of the redox-active pheophytin; D1-Tyr161, Tyr_Z; D1-Asp170, proposed to be involved in Mn binding; D1-His190, important for Tyr_Z or electron transfer to P_{680}; His198, proposed ligand to the central Mg^{2+} ion of the P_{680} chlorophyll; D1-His215 and D1-His272, ligands to the acceptor side Fe^{2+}. Shown in the lower part of the figure are the amino acid sequences for the D1 and D2 proteins in spinach. The α-helices are marked with bars above the sequences for the D1 protein and below the sequences for the D2 protein. The two helices in the C−D and D−E loops are marked with dashed bars. Residues conserved between the D1 and D2 proteins are shown in boldface.

calculations using the CHARMM program (Brooks et al., 1983). The form of the energy function is described in detail in Smith and Karplus (1992). The CHARMM version 22 protein topology and parameter files with all atoms explicitly included were used. Nonbonded interactions were smoothly truncated by a cubic switching function from 10 to 12 Å during energy minimization and from 7.5 to 8 Å during conformational searches.

Force Field Parameters for the Cofactors. Suitable parameters for the energy function, describing the reference values and force constants for the cofactor molecules (chlorophyll, pheophytin, and Fe^{2+}) bound in PSII, were lacking. It was therefore necessary to derive such parameters. The approach used to derive the parameters was similar to that adopted previously for bacteriochlorophyll and bacteriopheophytin (Foloppe et al., 1992, 1995). Partial point charges for the porphyrins were derived from semiempirical quantum mechanical calculations on an isolated molecule of the pheophytin analogue methyl pheophorbide *a* in two different crystallographically determined geometries (Fisher et al., 1972; Takahashi et al., 1984) using MOPAC 6.0 with the AM1 Hamiltonian (Dewar et al., 1985) and Mulliken population analysis (Mulliken, 1955). The charges from the two calculations were averaged and scaled by a factor of 0.721 for consistency with charges in the CHARMM22 topology file. Partial charges for the phytyl tail were calculated in the same manner, using the geometry obtained in the *Rps. viridis* structure. For chlorophyll, partial charges were adapted from pheophytin. The central Mg^{2+} ion was given the sum of the charges from the two hydrogens bound to the pyrrole nitrogens.

Bond length, bond angle, and dihedral angle reference values for the energy function were assigned the values in high-resolution crystallographic structures of chlorophyll and pheophytin analogues (Fisher et al., 1972; Chow et al., 1975; Kratsky & Dunitz, 1975, 1977; Takahashi et al., 1984). The force constants were derived by, as far as possible, transferring the existing parameters for the porphyrin macrocycle of the heme group (Kuczera et al., 1990). Force constants for the ring substituents were transferred from smaller, chemically related molecules (Smith & Karplus, 1992).

The isolated pigments were energy minimized starting from the crystallographic coordinates to an RMS energy gradient $<10^{-6}$ kcal mol^{-1} $Å^{-1}$. For methyl pheophorbide *a* the resulting heavy-atom RMS coordinate deviation between the crystallographic structure and the energy-minimized structure was 0.66 Å. The RMS deviation for the macrocyclic core was only 0.12 Å.

The energy function and parameters used to represent the coordination of the Mg^{2+} ion in the chlorophylls was that described in Foloppe et al. (1995). The Mg^{2+} to His bond distance of 2.13 Å was taken from a high-resolution crystal structure of a bacteriochlorophyll *a* binding antenna protein (Tronrud et al., 1986). The reference distance of 2.14 Å for the acceptor side Fe^{2+} and its histidine ligands was taken from the *Rps. viridis* structure. The force constants of 65 kcal mol^{-1} $Å^{-2}$ were taken from the Fe−His interaction in myoglobin (Kuczera et al., 1990).

Model System for Molecular Mechanics Calculations. Since only fragments of the D1 and D2 proteins are included in the model, the N-terminal and C-terminal ends of each segment were blocked with ammonium groups (D1-Leu106, D1-Asn266, D2-Cys106, and D2-Ser263) and carboxyl groups (D1-Ile224, D1-Leu297, D2-Phe224, and D2-Leu294). All side chains except D1-Glu130, D1-Asp170, and D1-Glu189 were assumed to be in their most common protonation states at pH 7 in aqueous solution. D1-Glu130 was protonated at the Oϵ1 position. This is similar to the situation in the *Rps. viridis* reaction center and is suggested from experimental results in PSII that indicate the presence of a D1-Glu130 hydrogen bond to the redox-active pheophytin (Lubitz et al., 1989; Moënne-Loccoz et al., 1989; Nabedryk et al., 1990). The side chains of D1-Asp170 and D1-Glu189 are close in space (Svensson et al., 1991). D1-Asp170 is known to affect manganese binding to the oxygen-evolving complex (Nixon & Diner, 1992; Chu et al., 1995a), raising the possibility that Mn ions coordinate to D1-Asp170. No Mn ions were included in the model. Therefore, to compensate for the absence of potential counterions for D1-Asp170 and D1-Glu189, these groups were protonated in the model. The histidines in the model are all assumed to be neutral with one proton on the Nδ1 position.

Amino acid substitution to or from prolines will locally affect the backbone conformation. There are seven non-proline and four proline residues in *Rps. viridis* that in PSII are respectively substituted to prolines and non-prolines (Table 1). In addition, there is a deletion of one residue in both the D1 and D2 proteins compared to the L and M

Table 1: Amino Acid Substitution Involving Prolines between *Rps. viridis* and PSII in the Modeled Region

Rps. viridis	PSII	*Rps. viridis*	PSII
Leu-L85	D1-Pro111	Ala-M151	D2-Pro150
Trp-L115	D1-Pro141	Val-M173	D2-Pro172
Pro-L118	D1-Ala144	Pro-M174	D2-Ser173
Ala-L237	D1-Pro279	Pro-M179	D2-Ala178
Pro-L253	D1-Phe295	Ser-M271	D2-Pro276
Thr-M142	D2-Pro141		

subunits of *Rps. viridis*. This deletion is located in the loop connecting the short CD helix and the D helix (Figure 1). This loop is flexible and adapts to the deletion without distorting neighboring α-helical structures. Backbone geometries in the regions of the proline exchanges and the deletion were regularized by limited energy minimization.

Different PSII cofactor compositions were tested in the calculations. The transfer from *Rps. viridis* of two or four chlorophylls, two pheophytins, and a Fe^{2+} ion was found to be possible without steric hindrance. However, a carotenoid placed in the same position as in the *Rps. viridis* reaction center was found to collide with D2-Phe158 and D2-Ala116, thereby increasing the van der Waals interaction energy unacceptably. The corresponding residues in *Rps. viridis* are both glycines. This suggests that the carotenoid binding in PSII might be significantly different from that in *Rps. viridis*. This might have functional relevance since P_{680}^+ would be able to extract electrons from a closely located carotenoid. In the *Rps. viridis* reaction center the carotenoid is bound close to the bacteriochlorophylls of the special pair. However, carotenoid oxidation is a rare event in PSII (Telfer et al., 1991), indicating that the binding site of the carotenoid probably is found further away from P_{680}.

Potential Energy Calculations and Rigid Rotation Conformational Searches. Energy calculations with CHARMM were applied to identify residues that had not adopted an optimal conformation. The internal self energy and the interaction energy with the environment were calculated for each residue and compared with the average values found for each residue type. The side chains of residues with above-average energies were positioned using rigid rotation torsional energy maps (Summers & Karplus, 1989). These maps are created by calculating the energy as a function of the dihedral angles of the side chain while keeping the rest of the protein rigid. One to three dihedral angles were varied at a time, and they were sampled at 10° intervals. For each residue the energy minimum conformation was retained. In the cases where several residues were found to closely interact, this procedure was performed iteratively to convergence.

Optimization of the Chromophore Conformations. Within the protein structure, the pigment molecules can be positioned in various ways which would result in different absorption spectra. The absorption spectra of two chromophores are shifted apart when they are near enough for their electric dipole moments to interact. The distance and the angle between the pigments determine the strength of the interaction. We have optimized the position of the primary donor chromophores in their protein environments, and the different pigment conformations were evaluated with exciton interaction calculations (Pearlstein, 1991) to determine if the interaction would agree well with experimentally determined absorption spectra. These exciton calculations were based on the point−dipole approximation from (Pearlstein, 1991), which positions the transition dipoles at the center of the chlorophyll macrocycle. This relatively simple model seems to hold well for describing the interactions in the PSII reaction center since the distance between the pigments allows little overlap between the porphyrin π-orbitals. Also, there is no evidence for the involvement of charge transfer states in the absorption spectrum of PSII reaction centers [cf. Scherer and Fischer (1991)]. Pigment orientations which gave satisfactory results for the exciton interaction were incorporated into the model, and a limited CHARMM force field minimization of the protein and porphyrin ring substituents was performed (Svensson et al., 1995). It was found that displacement of the two pigments corresponding to the special pair in purple bacteria is sufficient to obtain agreement between the calculated exciton interaction energy and those determined from experimental spectra of P_{680} (Van Kan et al., 1990; Braun et al., 1990; Carbonera et al., 1994; Kwa et al., 1994). The solution found involves a 1.5 Å symmetric translation of the two chlorophylls in the dimer along an axis parallel to the membrane plane and the chlorophyll ring planes together with a rotation of 5.5° around the normals to the chlorophyll ring plane. The center to center distance is 10.1 Å and the angle between the Q_Y transitions is 152°, giving a total exciton interaction energy of 182 cm^{-1} for the two chlorophylls of the dimer. A final energy minimization was performed with the macrocycle heavy atoms fixed to an RMS energy gradient of 0.08 kcal mol^{-1} $Å^{-1}$.

Evaluation of the Structural Model. The final model was evaluated using the PROCHECK programs (Laskowskii et al., 1993). This is a check of the stereochemical quality of the protein structure and includes the Ramachandran plot (Ramachandran et al., 1963), side-chain torsion angle and hydrogen bond energy analysis, and a secondary structure assignment based on the method of Kabsch and Sander (1983). The stereochemical quality of the present model as determined by the analysis within the PROCHECK programs is equivalent to an X-ray structure of about 2.0 Å resolution. In the Ramachandran plot 83.5% of the non-glycine, non-proline residues have backbone conformations that are within the most favored regions, 14.1% of the residues are in the additional allowed region, 1.6% (four residues) are in the generously allowed regions, and only as few as two residues, D2-Gln107 and D2-Ser166, out of the 248 non-glycine, non-proline residues are in the disallowed regions. No bad contacts between nonbonded atoms are present. The hydrogen-bonding potential (standard deviation of 0.7 kcal/mol), the peptide bond planarity (7.6° standard deviation), and the Cα tetrahedral distortion (1.8° standard deviation) are all within the accepted ranges defined for these properties from well-refined X-ray structures. The side-chain torsion angle potentials with standard deviations around 10° were in the model better than in high-resolution crystal structures. For the protein backbone the deviation from the ideal values was as follows: for the bond distances 0.006 Å and for the bond angles 1.4° as compared with the equilibrium bond length and angles from the CHARMM22 force field.

The planarity of the macrocycles in the PSII model is in the same range as in the *Rps. viridis* reaction center. The chlorophylls of the P680 pair are slightly more bent than the monomeric chlorophylls and pheophytins. This is due to stronger interactions with the protein environment. In the

chlorophyll pair, the CBD atoms (see Figure 3) are approximately 8° out of plane while all other atoms are less than 5° out of plane. In both the chlorophyll and the pheophytin molecules, the atoms of the partially saturated rings are found somewhat more out of plane than those of the unsaturated rings. In the dimeric chlorophylls, the central Mg^{2+} ions are displaced 0.2 Å out of the macrocycle plane toward the histidine ligands while the Mg^{2+} ions of the monomeric chlorophylls are found in the plane of the pyrrole nitrogens. This difference is due to the lack of protein ligands for Mg^{2+} in the monomeric chlorophylls in our model.

Empty spaces in the model large enough to accommodate solvent molecules or possibly other nonincluded cofactors were analyzed using the QUANTA 4.0 molecular modeling package (Molecular Simulation Inc., Burlington, MA). In the central part of the PSII model, the side chains together with cofactors are densely packed. Some empty spaces were found though. These could be sites for water molecules within the protein structure. The most dominant empty spaces were in the clefts between the D1 and D2 proteins, close to the monomeric chlorophylls. For this region, the structural prediction is weaker. Therefore, possible errors in the positioning of the monomeric chlorophylls, especially of the flexible phytyl tail, could partially be the cause of the empty spaces. Another possibility is that these empty spaces are part of the carotenoid binding sites in the PSII reaction center.

The PSII model was compared with the *Rps. viridis* structure using least squares fitting of the backbone coordinates using the McLachlan algorithm (McLachlan, 1982) as implemented in the program ProFit V1.6 (Dr. Andrew C. R. Martin, SciTech Software/UCL, http://www.biochem.ucl.ac.uk/~martin/#profit). The backbone coordinate RMS deviation is 1.75 Å. On the lumenal end of the B helix, the stromal end of the D helix, and both ends of the E helix, there are relatively large coordinate deviations from the purple bacterial structure. This may be related to the lack of the connecting loops and the long C-terminus. Another significant contribution to the coordinate RMS deviation comes from positions where prolines were interchanged with non-prolines (Table 1). Deviations are less in the interior of the structure where the cofactors are bound. The backbone coordinate RMS deviation of 1.75 Å between the PSII model and the *Rps. viridis* reaction center is in the range of what is expected for the protein core of two homologous proteins with a sequence identity of 20−25% (Hilbert et al., 1993).

It should also be pointed out that, although we have given the distances with 0.1 Å accuracy, the overall structural accuracy probably is lower than this, especially since the thermal fluctuations in proteins are on the 1 Å scale at physiological temperatures. The true reliability in the model is difficult to assess. This is the reason that no error bars are provided to the distances given.

The model was also compared with a previously published model for PSII (Ruffle et al., 1992) using QUANTA and ProFit, respectively, for graphical and computational analysis. The two models were superposed using the least squares fit of the backbone coordinates in the common structural region (D1-Gly110 to D1-Ala224, D1-Asn266 to D1-Met293, D2-Cys106 to D2-Phe224, D2-Ser263 to D2-Leu294). A coordinate RMS deviation was calculated for all heavy atoms for the same region but excluding position 122 on the D2 protein, which is not conserved between spinach (alanine) and pea (glycine). Coordinate RMS deviations were also calculated for the cofactors (four chlorophylls, two pheophytins, and the acceptor side Fe^{2+}).

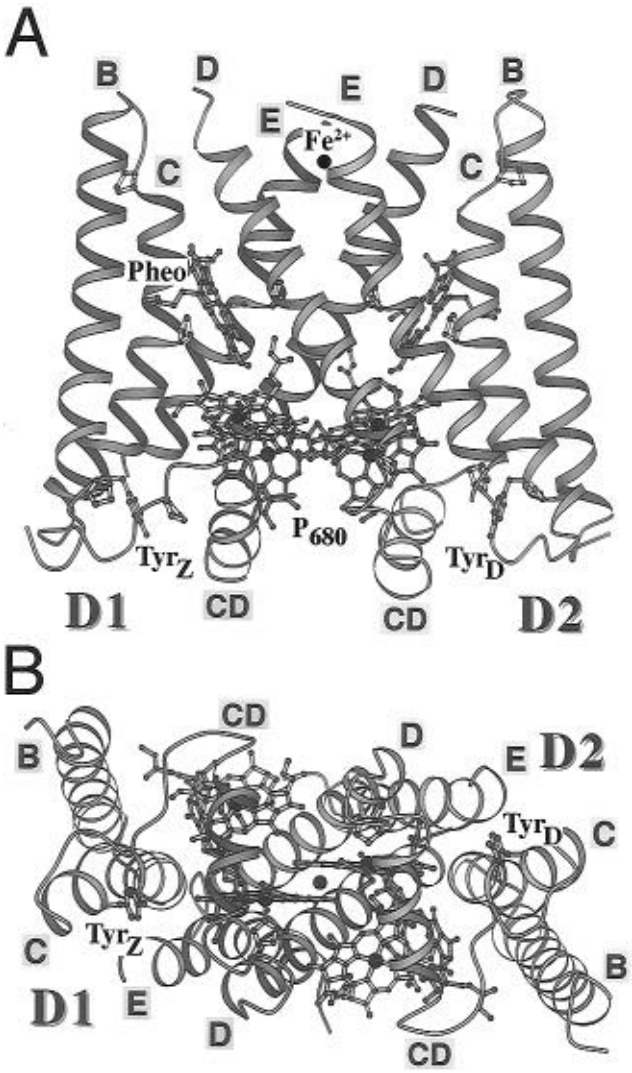

FIGURE 2: Overall structure for the PSII model. (A) A view within the membrane plane. Ribbon representations are drawn for the D1 protein (red) on the left and the D2 protein (blue) on the right. The redox components, the four chlorophylls, the two pheophytins, the tyrosine radicals Tyr_D and Tyr_Z, and the metal ions are shown as ball-and-stick representation. The phytyl chains are omitted for clarity. Also shown are the structurally important proline residues. (B) A view from the lumenal side of the thylakoid membrane down the axis between the center point of the chlorophyll dimer and the acceptor side Fe^{2+} ion. The D1 protein is on the left side and the D2 protein on the right. The symmetric position of the tyrosine radicals and the chlorophyll dimer constituting P_{680} is clearly visible. The figure was created with the program MOLSCRIPT (Kraulis, 1991).

RESULTS AND DISCUSSION

(I) Structure of the PSII Reaction Center. Our structural model of the PSII reaction center contains the central parts of the D1 and D2 proteins and bound cofactors (Figure 2A). In these regions, the D1 and D2 proteins are mainly in an α-helical conformation. In each protein there are four long, mostly hydrophobic membrane-spanning α-helices (B, C, D, and E). There is also a shorter helix on the lumenal side of the membrane between the transmembrane helices C and D, called the CD helix. This helix is partially in the membrane

Table 2: Secondary Structural Features Assigned from the Model Coordinates Using the Modified Kabsch and Sander (1983) Analysis Method Implemented in PROCHECK

	from	to	from	to
α-helix B	D1-Pro111	D1-Arg136	D2-Gly110	D2-Arg135
α-helix C	D1-Trp142	D1-Gln165	D2-Tyr142	D2-Gln165
α-helix CD	D1-Gly178	D1-Glu189	D2-Ile179	D2-Phe189
α-helix D	D1-Pro196	D1-Ser221	D2-Pro196	D2-Asn221
α-helix E	D1-Ser270	D1-Ile290	D2-Lys265	D2-Val288

Table 3: Angles between Helices of the D1 and D2 Proteins and the *C*2 Symmetry Axis

helix	D1, angle with *C*2 (deg)	D2, angle with *C*2 (deg)
B	15	15
C lumen	24	24
C stroma	0	1
D lumen	40	41
D stroma	28	29
E lumen	30	29
E stroma	19	14

layer and is amphipathic, with the more polar side facing the lumenal surface. The membrane-spanning helices are between 20 and 26 residues long. The secondary structural features are described in Table 2.

Helices C and E on both the D1 and D2 proteins contain proline residues in the center of the membrane-spanning region. Prolines may introduce a kink or a bending of an α-helix as well as exposing the backbone carbonyl (von Heijne, 1991). In the PSII model, the prolines that are within the transmembrane helices are all near the helix kinks. They face the interior of the protein and cause therefore a narrowing of the helix packing in the middle of the transmembrane segment. The kinked helices (Table 3) result in different helix packing on each side of the membrane. On the lumenal side, each transmembrane helix makes contacts only with nearest-neighbor helices on the same subunit. On the stromal side, the helix packing is more dense and close interactions exist between helices D and E on the D1 protein and helices D and E on the D2 protein (Figure 2A). Proline residues are also positioned at the start of helices B, C, and D and at the end of helix C on the D1 protein. On the D2 protein, prolines are positioned at the start of helices C and D and at the end of helix C. A proline in the first three positions of a helix stabilizes its formation since a *trans*-proline favors a helical backbone angle and also introduces rigidity of the protein backbone (MacArthur & Thornton, 1991). The prolines at the end points of the C helices function as helix breakers (Chou & Fasman, 1974), not allowing α-helical hydrogen bonding.

The modeled region contains 33 glycine residues, of which 10 are conserved between the D1 and D2 proteins. Several of these are positioned in the D and E helices at the middle of the transmembrane segment, allowing for dense helix packing. Several more of the glycines in the model are conserved with respect to the *Rps. viridis* reaction center and are located at or close to ends of α-helices (Michel & Deisenhofer, 1988). Their conservation provides further evidence supporting the structural homology of the two systems and was of crucial importance for their alignment (Michel & Deisenhofer, 1988).

Clustering of aromatic residues at the interface between the hydrophobic and hydrophilic parts of the membrane has been observed in membrane-bound proteins such as porins (Weiss et al., 1991; Cowan et al., 1992), bacteriorhodopsin (Henderson et al., 1990), and the purple bacterial reaction centers (Deisenhofer & Michel, 1989). It has been proposed that the aromatic side chains interact with the lipid headgroups and that the amphipathic nature of tyrosines and tryptophans could energetically stabilize the interface between apolar and polar environments (Cowan et al., 1992).

Aromatic residues are numerous in the PSII reaction center. However, in the PSII model there is no obvious clustering of phenylalanines, tyrosines, and tryptophans at the membrane surface interface. Only on the lumenal side is there a slight preponderance of aromatic residues. This difference between the D1 and D2 proteins and other membrane proteins might reflect the fact that the D1/D2 heterodimer has very little or no contact with lipids since it is surrounded by other proteins in the PSII complex. Alternatively, it may be due to the particular lipid content in the thylakoid membrane, which is dominated by galactolipids. The aromatic amino acids included in the D1 and D2 protein model are often involved in protein−cofactor interaction with ring structures of the chlorophylls and pheophytins (Figure 4A−C) or directly involved in electron transfer (Tyr_Z and Tyr_D) (Figure 4E,F).

Polar or charged amino acids are mostly found outside the membranous part of a transmembrane protein. However, there are several charged amino acids in the hydrophobic part of the D1/D2 heterodimer model. In all cases these are involved in liganding the cofactors (see below).

(II) Chromophore Composition and Binding. The PSII model includes four chlorophylls, two pheophytins, and a Fe^{2+} ion. This is similar to the purple bacterial reaction centers, which bind a bacteriochlorophyll dimer, two monomeric bacteriochlorophylls, two bacteriopheophytins, two quinones, and a non-heme Fe^{2+} ion. The cofactors and also the electron transfer rates between the primary donor and the electron acceptor system are comparable between PSII and purple bacteria (Rutherford, 1989; Diner et al., 1991b). Therefore, similar orientations and distances between the cofactors are expected, and for the acceptor side, the structural analogy between purple bacteria and PSII is almost complete. In contrast, there are large differences on the donor side.

Striking differences between PSII and purple bacteria are found in the function, orientation, and binding of the chlorophylls constituting the primary donor and the accessory chlorophylls. The exciton coupling between pigments in the entire PSII core complex is significantly lower than in the purple bacterial counterparts (Van Gorkom & Schelvis, 1993; Durrant et al., 1995), suggesting that the chromophore conformation is different. The orientations of the chlorophyll pigments in PSII are a subject of controversy (Diner & Babcock, 1996, and references therein), and several possibilities have been put forward. For example, recently two alternative models, derived originally from EPR measurements (Van Mieghem et al., 1991), were discussed in relation to absorbance difference spectra (Hillmann et al., 1995). In one of these models an accessory chlorophyll makes an angle of 30° with the membrane plane. In the other, one of the special pair chlorophylls makes an angle of 30° with the membrane plane. Electrochromic measurements have been interpreted as indicating that the special pair is formed from two, orthogonally oriented chlorophyll molecules (Mulkid-

Table 4: Center to Center Distances between Important Components in the Structural Model of PSII

	$Chl_{D2,acc}$	$Chl_{D1,P680}$	$Chl_{D2,P680}$	$Chl_{D1,acc}$	$Pheo_{D2,inact}$	$Pheo_{D1,act}$	Fe^{2+}	Tyr_Z	Tyr_D	D170
$Chl^{D2,acc}$		12.4	9.4	19.8	11.5	23.1	26.6	24.9	17.5	27.9
$Chl^{D1,P680}$			10.1	9.9	20.5	16.3	28.3	13.6	23.1	16.7
$Chl_{D2,P680}$				14.1	16.1	20.5	28.2	23.2	13.4	24.8
$Chl_{D1,acc}$					24.1	10.4	26.5	16.3	26.5	19.0
$Pheo_{D2,inact}$						23.1	18.4	33.3	21.7	37.2
$Pheo_{D1,act}$							18.3	21.9	32.9	26.4
Fe^{2+}								37.5	36.9	42.6
Tyr_Z									35.0	6.3
Tyr_D										35.2
D170										

janian et al., 1996) with the accessory chlorophyll on the D1 protein oriented perpendicular to the membrane. These three structural propositions are clearly qualitatively different.

To reconcile the various spectroscopic data on the primary donor in PSII, a deeper understanding of the relation to structure of the photophysics concerned may be required. Meanwhile, a more empirical approach can be taken in which proposed pigment geometries are incorporated into a detailed three-dimensional model of the protein which can then be tested by mutagenesis experiments. The approach we have taken was to use exciton interaction calculations in combination with potential energy calculations of the protein−pigment complex to test many different chlorophyll conformations that would fit the spectroscopic data to see whether they are structurally possible within the framework of the PSII model (Svensson et al., 1995). We have found that the primary donor in PSII might be constituted by two symmetrically placed chlorophyll molecules, as is the case in purple bacteria. However, the center to center distance of the chlorophylls in the pair is larger, with a separation of 10.1 Å (Table 4, Figure 4B) as compared to the distance of 7.3 Å in the *Rps. viridis* structure. The two monomeric chlorophylls are similarly placed and oriented as their purple bacterial counterparts.

Whereas adoption of pigment orientations radically different from the bacterial reaction centers cannot be ruled out, they cannot be incorporated without major rearrangement of the protein structure. Modeling such structural rearrangements is beyond the scope of the techniques applied here. Moreover, the present model is in accord with a number of experimental data concerning the donor-side structure, particularly the interactions of Tyr_D (see below). The construction of a protein model in which these interactions are preserved and in which the special pair chlorophylls are oriented in ways radically different from the present model (for example, orthogonal) would appear to be difficult. We therefore strongly favor a separated dimer structure for P_{680}, where the special pair is parallel and the accessory chlorophylls are tilted at 30° with respect to the membrane plane. The parallel conformation of the primary donor chlorophylls of PSII is supported also by the fact that the histidines ligating the central Mg^{2+} ion of the bacteriochlorophylls in the purple bacteria are preserved as D1-His198 and D2-His198 in PSII.

Our interpretation of the available spectra for the PSII reaction center is that chlorophylls with considerable excitonic interaction with P_{680} and chlorophylls with very weak interaction are both present in the reaction center. This can be explained only by PSII reaction centers containing five to six chlorophylls per two pheophytins, with two accessory chlorophylls close to the P_{680} and two bound more distant. Generally, PSII reaction center preparations bind four to six chlorophylls, two pheophytins, one to two β-carotenes, and one Fe^{2+} ion (Satoh, 1993; Seibert, 1993). Recent results suggest the presence of six chlorophylls per two pheophytins in most preparations (Eijckelhoff & Dekker, 1995). However, the functionally limiting number of chlorophylls most likely is four because the primary charge separation in PSII reaction center preparations with varying chlorophyll composition is similar. Similar conclusions have also been reached from hole-burning experiments (Chang et al., 1994) and from data obtained from reaction centers with one peripheral chlorophyll removed by Cu-affinity chromatography (Vasha et al., 1995).

The closely coupled pigments are most probably bound in the cleft between the D1 and D2 proteins, which corresponds to where the accessory pigments are bound in the purple bacteria. In the PSII model we have placed these pigments at the corresponding positions of the bacteriochlorophylls in *Rps. viridis* although the histidines coordinating the chlorophyll Mg^{2+} ions are not present in the D1 or the D2 proteins (Michel & Deisenhofer, 1988; Kuhn et al., 1994). It is possible that polar groups other than histidines can provide ligands to the Mg^{2+} ions of the accessory chlorophylls, since mutation of these histidines to serines in *Rb. capsulatus* has been made without any detected change in pigment composition or photosynthetic function (Coleman & Youvan, 1990). In antenna proteins many other groups can provide ligands to chlorophyll (Tronrud et al., 1986; Kühlbrandt et al., 1994). Possibly even water might be present as a ligand in PSII. However, this possibility cannot be addressed in the present modeling.

In addition to the inner chromophores corresponding to those in purple bacteria, there are often two extra chlorophyll *a* molecules bound to the PSII reaction center, making six chlorophylls per two pheophytins. These extra chlorophylls might be bound by D1-His118 and D2-His118 on the B helices as proposed by Michel and Deisenhofer (1988). This is supported by a mutation of the residue D2-His117 to tyrosine in *Synechocystis* 6803 (corresponding to D2-His118 in spinach), which resulted in loss of photosynthetic growth (Pakrasi & Vermaas, 1992). Chlorophylls bound at D2-His118 would in our model be oriented perpendicular to the membrane plane due to constraints in the protein structure. This orientation is supported experimentally by the finding that at least some of the accessory pigments in the PSII reaction center are almost perpendicular to the membrane plane (Kwa et al., 1992). These outer pigments are not involved in the primary charge separation (Schelvis et al., 1994), and they show a slow energy transfer to P_{680} of 10−50 ps (Schelvis et al., 1994; Vasha et al., 1995).

The additional two chlorophylls present in the PSII reaction center were not structurally included in our modeling, since the B helices on both the D1 and D2 proteins are on the periphery of our defined core structure and would have considerable interaction with other, nonhomologous protein regions that could not be included. These interacting, nonincluded protein regions are the A helices of the D1 and D2 proteins and possibly portions of the cytochrome *b*559, PsbI, PsbW, and/or the CP47 and CP43 proteins. A close interaction with the CP47 is highly likely since this is the antenna protein with the strongest association to the D1/D2 reaction center PSII (Ghanotakis et al., 1989).

(III) Detailed Description of Important Structural Elements. We have focused our analysis on the environments of the central redox components in the PSII reaction center core, *i.e.*, P_{680}, the redox-active pheophytin, the acceptor-side Fe^{2+}, and the tyrosine radicals, Tyr_D and Tyr_Z. Less well defined regions in the model include the binding sites of monomeric chlorophylls, the quinones, the carotenoids, and the Mn cluster, for which the sites in the model are only partial.

(i) P_{680}. The primary donor P_{680} is, in the model, constituted by two parallel chlorophylls symmetrically bound between the D1 and D2 proteins, toward the lumenal side of the membrane. Our optimization of the pigment positions in PSII shows that it is possible to accommodate two chlorophylls in a weakly coupled pair in the structural model of PSII (Svensson et al., 1995). The chlorophylls of the pair are separated by 10.1 Å, center to center distance, and nearly parallel, with the distance between the ring planes of 3.4 Å. Of the two chlorophylls in the pair, one is bound to the D1 protein, where D1-His198 provides a ligand to the central Mg^{2+} ion. The other is associated with the D2 protein and ligated by D2-His198. Due to the interaction with the histidine ligands the Mg^{2+} ions are pulled 0.2 Å out of the macrocycle planes.

Interestingly, after the two chlorophylls were moved apart to fulfill the exciton interactions (Svensson et al., 1995), new specific protein−chromophore interactions appeared in the structural model. Polar groups on the D1 and D2 proteins came close enough to the chlorophyll molecules to form hydrogen bonds. The hydrogen bonds are formed between D1-Thr286 and the O1D oxygen atom (PDB nomenclature, see Figure 3) of the 13^2 ester group (IUPAC, 1987) in $Chl_{D1,P680}$ and between D2-Ser283 and the corresponding oxygen on $Chl_{D2,P680}$ in the dimer (Figure 4A). The hydrogen bond distances are 2.7 and 2.6 Å, respectively. Another implicated protein−pigment interaction of importance is a close van der Waals contact between D2-Trp192 and the D2-associated chlorophyll of the dimer ($Chl_{D2,P680}$). This tryptophan is stacked against ring D of the chlorophyll and interacts possibly via a weak hydrogen bond to the O2D oxygen of the 13^2 ester group of $Chl_{D2,P680}$. This arrangement is in accord with results from FTIR experiments, indicating the presence of at least two, probably three, hydrogen bonds between the chlorophylls in P_{680} and the protein (Nogushi et al., 1993).

The hydrogen bonds to the chlorophylls are interesting, since hydrogen bonds are known to modify the redox potential of the special pair in purple bacteria (Williams et al., 1992; Stocker et al., 1992; Wachtveitl et al., 1993). However, in the purple bacteria the hydrogen bond is formed

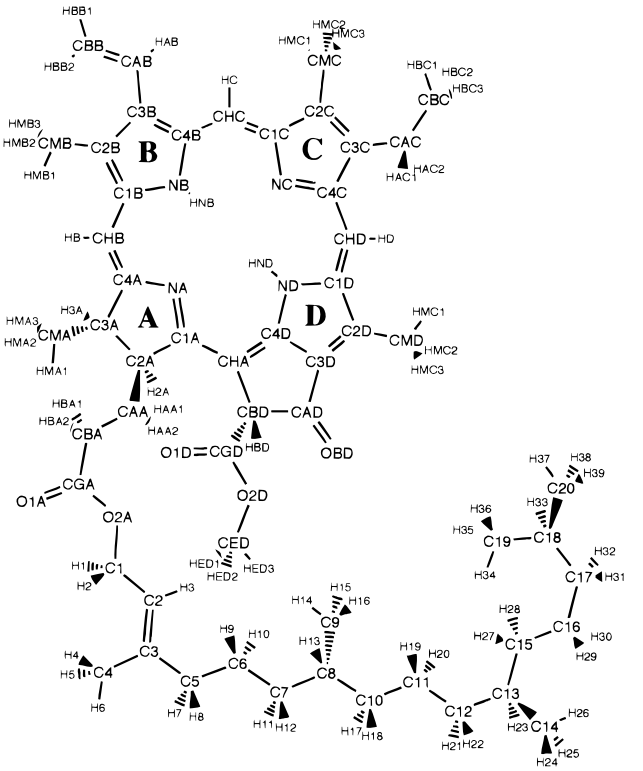

FIGURE 3: Chemical structure of pheophytin *a*. Atom names are according to the Brookhaven Protein Database (PDB) guidelines on tetrapyrrole nomenclature.

with the bacteriochlorophyll acetyl group, which is conjugated with the macrocyclic ring. This group corresponds to a vinyl group in chlorophyll *a*, which cannot be involved in hydrogen bonding. The hydrogen bonds we have suggested are not conjugated to the macrocycle, which might suggest that they have little effect on the redox potential of P_{680}. Instead, they probably have a structural role in binding and orienting the pigment molecules.

From the analogy with purple bacteria, D1-His198 and D2-His198 have been suggested to coordinate the chlorophylls of P_{680} (Trebst, 1986; Michel & Deisenhofer, 1988). Some experimental support for this hypothesis comes from mutagenesis work in *Synechocystis* 6803. In the mutant D2-His197 → Tyr or Leu (sequence position corresponds to D2-His198 in spinach) the PSII complex was not assembled or perhaps destabilized (Vermaas et al., 1987; Pakrasi & Vermaas, 1992). The result was similar for the mutation D1-His198 → Leu (Diner et al., 1991a). Mutants with D2-His197 → Gln or Asn could be grown photoautotrophically. The function of PSII was somewhat impaired, which in D2-His197 → Gln could be explained by a lowered midpoint potential of the P_{680}/P_{680}^+ redox couple (Vermaas, 1993). These results support the function of D1-His198 and D2-His198 as ligands to P_{680}. Interestingly, mutations of the corresponding residues His M200 → Leu or Phe and His-L173 → Leu in *Rhodobacter capsulatus* resulted in a reaction center with a heterodimeric special pair containing a bacteriochlorophyll and a bacteriopheophytin (Coleman & Youvan, 1990). The binding of pheophytin instead of chlorophyll could not be achieved in PSII since the PSII complex seems to be more sensitive than purple bacteria to changes in this region. This could be explained if one assumes that the stability of the D1 or D2 proteins is decreased when chlorophyll cannot be coordinated or that the binding of the

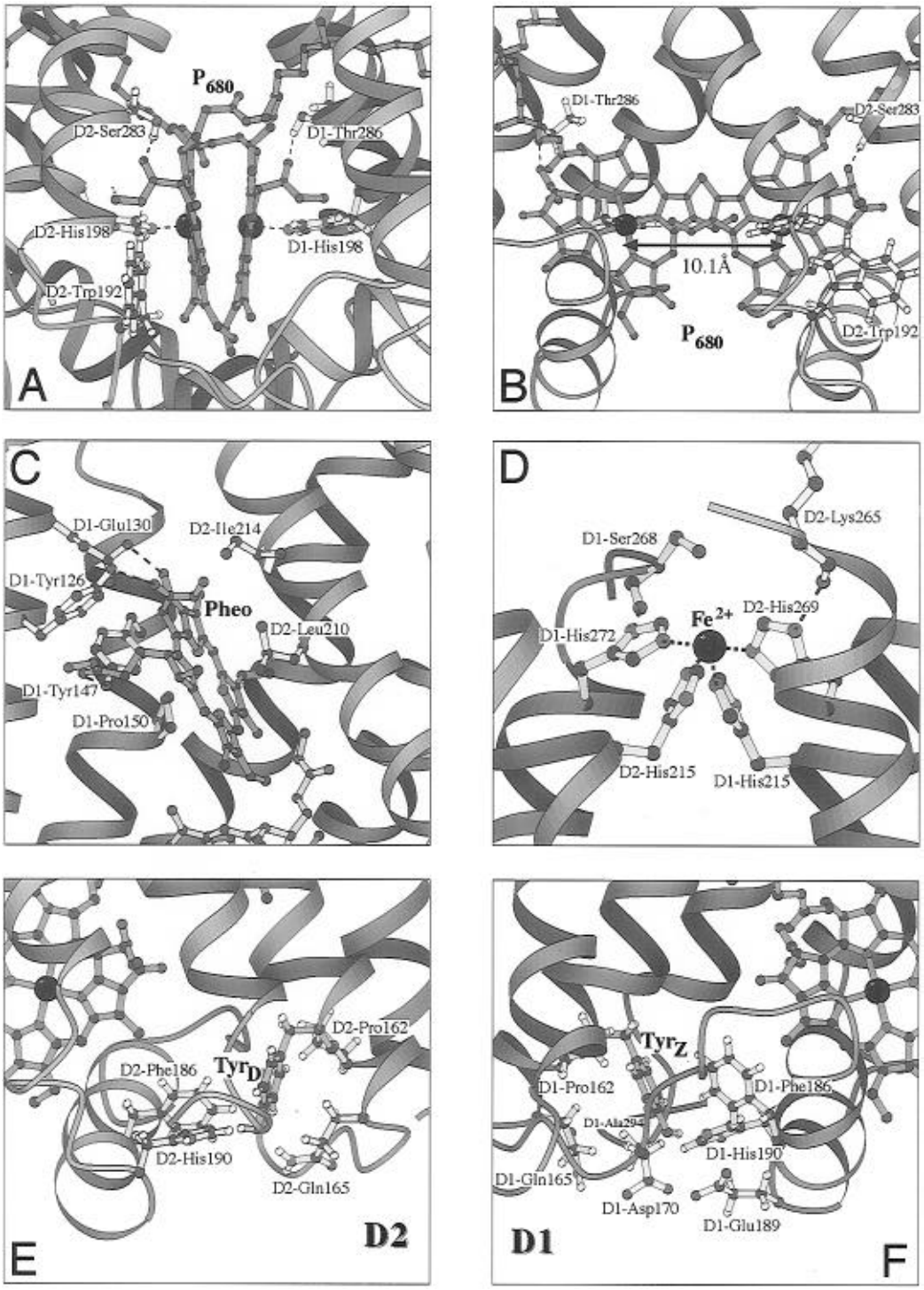

FIGURE 4: (A) Chlorophyll dimer proposed to constitute the primary donor, P_{680}, as derived by the structural fitting of the chlorophyll orientations on the basis of exciton interaction calculations. The view is in the membrane plane parallel to the chlorophyll ring planes. The D1 protein, on the right-hand side, provides two ligands to the $Chl_{D1,P680}$. D1-His198 is a ligand to the central Mg ion, and D1-Thr283 is hydrogen bonded to the O1D ester oxygen. On the left-hand side, the corresponding ligands from the D2 protein to $Chl_{D2,P680}$ are shown. D2-His198 coordinates the central Mg ion, and D2-Ser286 forms a hydrogen bond to the O1D ester oxygen. The figure also shows D2-Trp192, which is stacked against ring D of the chlorophyll and possibly hydrogen bonded to the O2D oxygen of $Chl_{D2,P680}$. (B) Chlorophyll dimer in a view perpendicular to the chlorophyll ring planes. The orientation is as in Figure 2A. The center to center distance between the chlorophylls in the model is 10.1 Å, giving a very small atomic overlap, which is considerably lower than for the special pair in a purple bacterial reaction center. (C) Structural environment of the pheophytin electron acceptor. The specific binding of the pheophytin is mostly defined by the hydrogen bond from D1-Glu130 (upper left). The carboxyl group of this residue points toward the carbonyl oxygen on the pheophytin macrocycle. D1-Tyr126 and D1-Tyr147 also provide hydrogen bonds to the pheophytin. Residues interacting with the macrocyclic ring are D1-Tyr147 and D1-Pro150 in the C helix. On the other side of the ring, the side chain of D2-Leu210 is packed at van der Waals distance, and toward the acceptor side we find residue D2-Ile214. The orientation is similar to that in Figure 2A. (D) Acceptor side iron with its four histidine ligands: D1-His215, D1-His272, D2-His215, and D2-His269. The interactions between the histidines and the Fe^{2+} ion are indicated with dashed lines. The stromal ends of helices D and E from both the D1 (behind) and D2 (in front) proteins are shown. Other residues shown are D1-Ser268 and D2-Lys265, which, with their peptide oxygens, are proposed to be hydrogen bonded (dashed lines) to the Nδ nitrogens on D1-His272 and D2-His269, respectively. The orientation is as in Figure 2A. (E) Structural environment of Tyr_D. This panel shows a part of the D2 protein with the plane of the membrane oriented perpendicular to the plane of the paper. The

chlorophylls is required for the formation of the D1/D2 reaction center complex.

In the PSII model, the P_{680} pair chlorophylls are in van der Waals contact with the accessory chlorophylls on the D1 and D2 side. This is similar to the purple bacterial structures but the interaction is substantially stronger. This results from the translations of the chlorophylls made in the exciton interaction optimization, where the pair pigments were moved away from each other. As a result they slightly approached the accessory pigments (Svensson et al., 1995). The contacts are edge to side with a center to center distance for the chlorophylls of approximately 10 Å (Table 4). Many residues constitute the binding pocket for the chlorophylls. Most interact principally via van der Waals energies. A few significant electrostatic interactions are also found. D1-Met183 interacts electrostatically with the nitrogens and the Mg^{2+} ion of the $Chl_{D1,P680}$. D1-Met183 is positioned on the opposite side of the liganding D1-His198. D1-Gln187 is in van der Waals contact with the ethyl ring substituents and possibly also forms hydrogen-bonding interactions with D1-Met293 and D1-His195, which are close to, but not in contact with, $Chl_{D1,P680}$. The residue D1-His195 has been mutated in *Chlamydomonas reinhardtii* to asparagine, tyrosine, and aspartate. The result was a slightly lower oxygen evolution and a shifted equilibrium constant between $Tyr_ZP_{680}^+$ and $Tyr_Z^{ox}P_{680}$, most likely due to a change in the midpoint potential for the Tyr_Z/Tyr_Z^{ox} couple (Roffey et al., 1994a; Kramer et al., 1994). From the present model, as D1-His195 is closer to P_{680} than to Tyr_Z, we would suggest that the mutation rather affects P_{680} or the electron transfer between P_{680} and Tyr_Z.

In purple and green bacteria, Tyr-M210 is important for the charge separation and the electron transfer from the special pair to the bacteriopheophytin, and an exchange of Tyr-M210 → Phe slows down the reaction by a factor of 4 (Finkele et al., 1990). In *Chloroflexus aurantiacus* M210 is a leucine, and the primary electron transfer is considerably slower than in purple bacterial reaction centers (Becker et al., 1986). In PSII it has been suggested that D2-Leu206, which corresponds to M210 in purple bacteria, is responsible for the slower charge separation in the PSII reaction center (Barber, 1993). In the model, D2-Leu206 is located close to the accessory chlorophyll on the active branch and to both chlorophylls of the P_{680} pair. The corresponding residue on the inactive branch is D1-Phe206, which also is in van der Waals contact with both chlorophylls of the pair and the accessory chlorophyll.

(ii) The Pheophytins. The pheophytin electron acceptor is bound in the center of the hydrophobic membrane-spanning part of PSII between helix C of the D1 protein and helix D of the D2 protein (Figure 2A). In the model, the specific binding of the pheophytin is most prominent with D1-Glu130. The carboxyl group of D1-Glu130 forms a hydrogen bond to the carbonyl oxygen bound to the OBD position (Figure 3) (13^1 position, IUPAC) of the pheophytin macrocycle (Figure 4C). The distance from the carboxylic oxygen on D1-Glu130 to the carbonyl oxygen on the pheophytin is 2.58 Å. This coincides well with the expected bond length of 2.4−2.7 Å for a strong O−H···O hydrogen bond (Brown, 1976). The pheophytin is bound by two more hydrogen bonds provided by residues of the D1 protein. These residues, D1-Tyr126 and D1-Tyr147, are hydrogen bonding the ester group oxygens O1D and O1A, respectively (Figure 4C). In the close vicinity, D1-Arg129 is involved in a hydrogen bond to the phenolic oxygen of D1-Tyr126 and is within 5 Å of D1-Glu130 and the O1D position of the pheophytin. Also D2-Leu210 interacts with the pheophytin and is packed at van der Waals distance from the center of the macrocyclic ring. On the other side of the ring the aromatic side chains of D1-Tyr147 and the D1-Pro150 are very close. Toward the binding pocket of the quinone acceptor Q_A we find D1-Ile143 and D2-Ile214. Possibly important for the function of electron transfer is the phytyl tail from $Chl_{D1,P680}$ of the special pair, which is in van der Waals contact with the macrocycle of the pheophytin. The phytyl tail of the pheophytin stretches toward the lumenal side, spanning the distance to the special pair.

The orientation and predicted structure around the pheophytin acceptor in PSII are well conserved from the bacterial reaction center structures. This has been proposed earlier by independent experiments using different spectroscopic methods (Lubitz et al., 1989; Moënne-Loccoz et al., 1989; Nabedryk et al., 1990; Kwa et al., 1992). Measurements have revealed that the carbonyl oxygen at the 13^1 position on the pheophytin in PSII forms a hydrogen bond to a nearby carboxylic amino acid. This is similar to the situation in the purple bacterial reaction centers, and in the *Rps. viridis* reaction center this bond is formed to Glu-L104. Sequence alignment studies suggested that the corresponding residue in PSII was D1-Glu130 (Michel & Deisenhofer, 1988), which is supported in our energetically optimized structure (Figure 4C). Thus, both the spectroscopic (Lubitz et al., 1989; Moënne-Loccoz et al., 1989; Nabedryk et al., 1990) and the structural work presented here support the existence of the hydrogen bond to the pheophytin in PSII.

Further evidence comes from site-directed mutagenesis experiments. In the cyanobacterium *Synechocystis* 6803 residue 130 on the D1 protein is a glutamine. Mutation of D1-Gln130 to glutamate and leucine resulted in a modified quantum yield of the $P_{680}^+Pheo^-$ formation and a shift of the Q_X absorption band in the pheophytin spectrum (Giorgi et al., 1996). A more polar side chain at position 130 of the D1 protein gives a higher wavelength peak position, which seems to reflect the hydrogen-bonding strength. The hydrogen bond is strongest when a glutamate is present at position 130, weaker when there is a glutamine, and not there at all in the leucine mutant. Site-directed mutagenesis work of the corresponding residue Glu-L104 in purple bacteria has given comparable results (Bylina et al., 1988). Relevant to this is work on the cyanobacterium *Synechococcus* 7942.

protein backbone is drawn with ribbons for the helical regions and wires for the loop regions. In the center, drawn with orange-colored bonds is Tyr_D, D1-Tyr161. The side chains of D2-Pro162, D2-Gln165, D2-Phe186, and D2-His190 are shown. On the left-hand side, a part of the nearest chlorophyll of the P_{680} pair is visible. The orientation is as in Figure 2A. (F) Structural environment of Tyr_Z. This panel shows part of the D1 protein with the plane of the membrane oriented perpendicular to the plane of the paper. The protein backbone is drawn with ribbons for the helical regions and wires for the loop regions. In the center, drawn with orange-colored bonds is Tyr_Z, D1-Tyr161. The side chains of D1-Pro162, D1-Gln165, D1-Asp170, D1-Phe186, D1-Glu189, D1-His190, and D1-Ala294 are shown. On the right-hand side, a part of the nearest chlorophyll of the P_{680} pair is visible. The orientation is as in Figure 2A.

In this strain, two distinct forms of the D1 protein are expressed under different light conditions and show a different sensitivity to photoinhibition (Clarke et al., 1993a; Kulkarni & Golden, 1994) as well as a different photochemical yield (Clarke et al., 1993b). The most striking difference among the 25 differing amino acids between the two forms of the D1 protein is in position 130, which is a glutamic acid in the most efficient gene product and a glutamine in the other. These data could suggest the importance of hydrogen bonding in adjusting the redox potential to optimize function. Since the 13^1 (OBD) oxygen is part of the conjugated system of double bonds in the porphyrin macrocycle, it is expected that a modified interaction with this position will have a considerable effect on the electronic structure of the pheophytin. It is also known that mutations affecting the hydrogen-bonding influence the redox potentials of bacteriochlorophylls in the purple bacterial reaction center (Williams et al., 1992; Stocker et al., 1992; Wachtveitl et al., 1993) and the heme group in cytochrome *c* (Langen et al., 1992).

The other two hydrogen bonds that are proposed from the modeling are likely to have more structural roles in binding the pheophytin. D1-Tyr126 and D1-Tyr147 hydrogen bond to the ester groups which are more distant from the macrocyclic ring system. These residues are well conserved in all organisms. However, the cyanobacterium *Anabaena* 7120, which also has two gene forms encoding the D1 protein, possesses a phenylalanine at position 147 in form 2 and 3 of the D1 protein. It would be interesting to study the photochemical yield in this organism to verify the effect of the hydrogen bond from D1-Tyr147.

D2-Leu210 is conserved from the purple bacteria and corresponds to Leu-M212 in *Rps. viridis* and Leu-M214 in *Rh. sphaeroides*. The side-chain orientation is almost identical in our model and the crystallographic structures (Deisenhofer et al., 1985; Allen et al., 1987a,b). Leu-M214 has been mutated to a histidine in *Rb. sphaeroides* with the result that the bacteriopheophytin was replaced by a bacteriochlorophyll with the exchanged histidine side chain being a ligand to the central Mg ion (Chirino et al., 1994). Electron transfer was slowed down between the special pair and the bacteriopheophytin, and the quantum yield of Q_A^- formation was lowered (Kirmaier et al., 1991). It would be interesting to introduce similar changes by mutagenesis also in PSII.

Toward the proposed binding pocket for Q_A, we find the hydrophobic residues D1-Ile143 and D2-Ile214. Unfortunately, our model does not include other residues between the pheophytin and Q_A. The Q_A binding site is in part constituted by the D−E loop, which compared to the purple bacteria includes large insertions and therefore cannot be reliably modeled.

The pheophytin on the inactive branch is also bound strongly with several hydrogen bonds. The residue D2-Gln130 is involved. The amide nitrogen is the hydrogen bond donor to the pheophytin OBD position. It also donates a hydrogen bond to the O1D position of the pheophytin. D1-Tyr126, which binds the O1D position at the active branch, is not present in the D2 protein. Instead, we find a phenylalanine here, which is in van der Waals contact with this part of the pheophytin. Also at position 147 there is a phenylalanine in the D2 protein instead of the corresponding tyrosine in the D1 protein. The pheophytin O1A position lacks a hydrogen bond on the inactive branch, while there is one additional hydrogen bond to the OBD position coming from D2-Asn143. D1-Met214 is only 3.8 Å away from the OBD position and the macrocyclic ring of the inactive pheophytin. Interestingly, both D2-Asn143 and D1-Met214 are in the region which faces the quinone binding site of Q_B. On the other branch the corresponding residues are both isoleucines. Thus, the inactive branch is more hydrophilic toward the quinone site. Other residues making van der Waals contacts with the macrocycle of the pheophytin are D2-Phe147, D2-Pro150, and D1-Leu210. The phytyl tails of the chlorophylls on this branch are also in close contact with the macrocyclic ring of the pheophytin. To our knowledge no mutagenesis experiments have been done in this region of the PSII reaction center.

(iii) The Acceptor-Side Fe^{2+}. The nonheme Fe^{2+} ion on the acceptor side of PSII is bound to residues at the stromal ends of helices D and E of the D1 and D2 proteins (Figure 2A,B), where it is ligated by four histidines, D1-His215, D1-His272, D2-His215, and D2-His269, in the structural model (Figure 4D). These four histidines are conserved in all PSII sequences (Svensson et al., 1991). It has been proposed from EXAFS studies that histidines are involved in Fe^{2+} and quinone binding in PSII (Bunker et al., 1982). The pattern of the four histidine ligands was suggested from the similarity with the purple bacterial reaction center structures and their identity proposed from sequence analysis (Trebst, 1986; Michel et al., 1986; Michel & Deisenhofer, 1988). Spectroscopic studies indicate that the ligation of the Fe^{2+} ion is structurally very similar between purple bacteria and PSII (Diner & Petrouleas, 1987; Rutherford, 1987).

Other important residues in the modeled environment of the Fe^{2+} ion are D1-Ser268 and D2-Lys265, which with their peptide oxygens are hydrogen bonded to the Nδ nitrogens on D1-His272 and D2-His269, respectively. D1-Ser268 interacts electrostatically with the Fe^{2+} ion and its ligands. D1-Ser212, D2-Cys212, D2-Met272, and the peptide oxygen of D1-Leu271 interact electrostatically with the Fe^{2+} and its histidine ligands, toward the interior of the protein. Nonpolar residues including D1-Val219, D1-Leu275, and D2-Val219 constitute the close environment of the acceptor-side iron and its histidine ligands.

Experimental evidence for histidines coordinating the Fe^{2+} is provided from mutagenesis work on the cyanobacterium *Synechocystis* 6803, where D2-His268 (corresponding to D2-His269 in plants) has been mutated to a glutamine (Vermaas et al., 1994). The mutants lost photoautotrophic growth and did not show any electron transfer from Q_A to the plastoquinone pool, *i.e.*, Q_B. Both quinone pockets were perturbed, which could be explained by the loss of the nonheme iron. Other mutants in this region are D2-His214 → Asn and D2-Gly215 → Trp in *Synechocystis* 6803 (Vermaas et al., 1987, 1990a). These residues correspond to D2-His215 and D2-Gly216 in higher plants. Both of these mutations showed a destabilization of the D2 protein and disturbed the local structure around Q_A and Fe^{2+}.

Since the high-spin Fe^{2+} ion is expected to have one or two more ligands, there should be at least one further ligand to the iron in PSII. This ligand cannot be predicted from the model since the loop regions on the stromal side, which could hold the last ion ligand (see below), are not in our included region (Figure 1). In purple bacteria the last two ligands come from a glutamate residue, Glu-M232 in *Rps. viridis*, which functions as a bidentate ligand. This residue

is not conserved in PSII. Instead, the fifth ligand has been suggested to be a bicarbonate ion (Michel & Deisenhofer, 1988; Van Rensen et al., 1988), and there exists strong experimental evidence for this hypothesis from ligand displacement experiments (Petrouleas & Diner, 1990). The bicarbonate ion is proposed to bind as a carbamate to the D2-Lys265 amino group or with an ionic interaction with D2-Lys265 and D2-Arg266 (Diner et al., 1991b). Other residues interacting with HCO_3^- and modifying the bicarbonate effect have been suggested from mutagenesis work (Govindjee, 1993). These include several residues involved in herbicide resistance, of which only D1-Leu275 is included in the model. D1-Leu275 seems to be part of the Q_B binding site and is therefore not likely to directly affect either the Fe^{2+} or its ligands. In contrast to the bicarbonate hypothesis, D1-Glu231 has been proposed to be a direct ligand to the Fe^{2+} ion from modeling work by Ruffle et al. (1992).

The structural similarity between the PSII model and the purple bacterial structures is very high for the Fe^{2+}/quinone region, and we cannot directly localize the origin of the functional differences between PSII and purple bacteria: the lower redox midpotential of the Fe(III)/Fe(II) transition in PSII, the NO binding, or the pH dependence of the *g*-value of the Q_A^-Fe(II) EPR signal (Rutherford & Zimmermann, 1984; Diner et al., 1991b). However, it is possible that these differences are dependent on the fifth ligand (the HCO_3^-) and residues from the stromal loops of the D1 and D2 proteins that are not included in the model.

(iv) The Tyrosyl Radicals. The redox-active tyrosyl residues Tyr_D and Tyr_Z have been identified as Tyr161 on the D2 protein (Debus et al., 1988b; Vermaas et al., 1988) and Tyr161 on the D1 protein (Debus et al., 1988a; Metz et al., 1989), respectively. Tyr_D and Tyr_Z are located symmetrically relative to the *C*2 axis near the lumenal ends of helix C on the D2 and D1 proteins, respectively (Figure 2A). The symmetric location of the two tyrosyl radicals relative to the acceptor side Fe^{2+}, which is placed on the *C*2 axis, was recently experimentally supported by relaxation enhancement measurements (Koulougliotis et al., 1995). The distances from Tyr_D and Tyr_Z to the acceptor side Fe^{2+} are measured to be 37 ± 5 Å (Bosch et al., 1991; Hirsch & Brudvig, 1993; Koulougliotis et al., 1995), which agrees well with the distances derived from the model of 36.9 and 37.5 Å, respectively (Table 4). The tyrosine residues are located on the side of the C helix which faces the special pair. Their protein environments are constituted by residues from the C and D transmembrane helices, the lumenal C−D loop, and the CD helix (Figure 4E,F) (Svensson et al., 1991). The distance between the center of the ring of Tyr_D and Tyr_Z and the closest Mg atoms in the chlorophyll pair is 13−14 Å (Table 4). The distance between Tyr_Z and P_{680} has been estimated by EPR measurements to be 10−15 Å (Bock et al., 1988; Hoganson & Babcock, 1988) and 14 Å (Kodera et al., 1992), which agrees with the model. The experimentally obtained distance between Tyr_D and Tyr_Z of 30 Å (Astashkin et al., 1994) is slightly lower than the 35 Å that we see in our model (Table 4).

Tyr_D. The orientation of Tyr_D in the membrane has been studied by EPR spectroscopy (O'Malley et al., 1984; Rutherford, 1985; Un et al., 1994). The published orientation data have been interpreted as an angle of 55−65° between the radical C1−C4−phenolic oxygen axis and the membrane plane (Svensson et al., 1990). The tyrosyl ring plane has been suggested to form a 65−75° angle with the membrane plane (Un et al., 1994). In the present model, the orientation of Tyr_D is in agreement with the orientation from the EPR data, and the angle between the C1−C4−phenolic oxygen axis and the membrane plane is 67°. The phenolic oxygen is pointing toward the lumenal surface of the membrane (Svensson et al., 1990). This orientation was also the energetically most favorable for Tyr_D.

Furthermore, spectral simulation of the EPR signal from Tyr_D has provided information on the angle between the β-methylene protons and the $2p_z$ orbital of the Cγ (C1) carbon of the phenolic ring (Rigby et al., 1994; Tommos et al., 1994; Warncke et al., 1994). For the proton which couples most strongly with the unpaired electron of the phenolic ring, this angle in spinach is 48° (Rigby et al., 1994), and we have constrained the dihedral angle in our model to the corresponding angle. However, when we tried to energy minimize the model without these dihedral constraints, a very similar angle was found as determined experimentally.

Tyr_D is located in a hydrophobic environment constituted of many aromatic residues (Svensson et al., 1991). The most prominent interaction in the model is the hydrogen bond to D2-His190 (Figure 4E). The distance between the Nϵ1 nitrogen in the histidine and the phenolic oxygen in the tyrosine is 2.8 Å. That Tyr_D is hydrogen bonded is supported by ESEEM, ENDOR, and FTIR spectroscopic investigations (Rodriguez et al., 1987; Evelo et al., 1989a,b; Tang et al., 1993; Bernard et al., 1995). The close proximity between Tyr_D and a base, most probably a histidine, was also proposed from kinetic EPR data (Vass & Styring, 1991).

It is quite possible that D2-His190 also fulfills a structural role in connecting the C−D loop with the turn where the E helix breaks, by hydrogen bonding to the peptide oxygen of D2-Leu294 (Figure 4E). Another residue that interacts strongly with Tyr_D is D2-Gln165, which, with its amide group, comes close to the phenolic oxygen of the tyrosine to form another hydrogen bond (Figure 4E). In addition, Tyr_D is surrounded by many other conserved hydrophobic residues (D2-Phe170, D2-Phe182, D2-Phe189, D2-Leu290, and D2-Ala291). D2-Phe186, which is in van der Waals contact with the aromatic ring of Tyr_D, is part of the CD helix and occupies the space between Tyr_D and the primary donor, approximately midway between these. D2-Phe186 is not conserved between higher plants and cyanobacteria and is a leucine in the latter (Svensson et al., 1991). D2-Ala291 is in van der Waals contact with the aromatic ring of Tyr_D. Important for the spatial orientation of Tyr_D is D2-Pro162, the residue next in sequence on the same helix.

Important aspects of the model were recently verified by EPR spectroscopy of the Tyr_D^{ox} radical in the cyanobacterium *Synechocystis* 6803, where residues on the D2 protein predicted to interact with the Tyr_D^{ox} radical were mutated (Tommos et al., 1993, 1994; Tang et al., 1993). Modified EPR spectra have been published for the following mutants: D2-Pro161 → Ala, D2-Pro161 → Leu, D2-Gln164 → Leu, D2-His189 → Leu, D2-His189 → Tyr, D2-His189 → Asp, and D2-His189 → Glu (the residue numbering in the D2 protein of *Synechocystis* 6803 differs by one residue compared to spinach, due to a deletion at the N-terminus). The altered EPR spectra were, in the D2-Pro161 → Ala and D2-Gln164 → Leu mutants, found to be due to slight twists in the orientation of the radical ring plane (Tommos et al., 1994). In the first case, the twist is probably due to a slightly

perturbed backbone conformation imposed by the exchange of the proline residue. In the latter case the twist is due to different side-chain interactions induced by the mutation. In the mutants of D2-His189 the spectral change imposed by the mutation is much larger. The *g*-value is, as in the wild type, close to 2.0050 but the line width is much smaller. This indicates a major change in the close environment of Tyr_D. In this case the predicted hydrogen bond is probably lost, and it is also possible that the D2 protein structurally is perturbed due to removal of the hydrogen bond to the E-helix. High-field EPR on the mutant D2-His189 → Gln indicate that Tyr_D^{ox} is not hydrogen bonded or much weaker hydrogen bonded in this mutant (Un et al., 1996). The mutant work and the related EPR spectroscopic work around Tyr_D are strongly supportive for the structural model.

Tyr_Z. Tyr_Z has been predicted to be similarly oriented in the membrane as Tyr_D because of the similarity in the EPR spectrum of Tyr_Z^{ox} and Tyr_D^{ox} (Babcock & Sauer, 1973; Hoganson & Babcock, 1988). Recent EPR data on oriented samples have shown Tyr_D and Tyr_Z to be similarly oriented with the C−O bond approximately parallel to the membrane normal (Mino & Kawamori, 1994). Tyr_Z is placed in the structural model similarly as Tyr_D with the phenolic oxygen pointing toward the lumen. In contrast, Tyr_Z is found in a more flexible environment than Tyr_D (Mino & Kawamori, 1994), which is supported by the experimentally determined higher rotational mobility of the aromatic ring (Tommos et al., 1995). In addition, the relatively large similarity in the EPR spectra between Tyr_Z^{ox} and Tyr_D^{ox} indicates that the dihedral angle between the β-methylene protons and the $2p_z$ orbital of the Cγ (C1) carbon of the tyrosyl ring is very similar between the two radicals, and we have therefore, also for Tyr_Z, constrained the angle to 48° during the energy minimization.

Tyr_Z is in the model found in a much more hydrophilic environment than Tyr_D (Svensson et al., 1991). Toward the lumenal side from Tyr_Z there is a cluster of polar and charged residues: D1-Gln165, D1-Asp170, and D1-Glu189 (Figure 4F). They come close in space and might constitute part of the binding site for the Mn cluster within a few angstroms from Tyr_Z (Svensson et al., 1991). D1-Asp170 has been proposed to be involved in Mn binding (Nixon & Diner, 1992; Chu et al., 1995a). Recent data indicate that the distance between Tyr_Z and the Mn cluster might be as close as 4.5 Å (Gilchrist et al., 1995). Considering our structural model, a Mn ion that close to Tyr_Z most likely is coordinated by D1-Asp170. Highly relevant for the structural considerations is also a mechanistic model that recently was proposed, where Tyr_Z^{ox} acts as an hydrogen atom abstractor directly coupled to the water splitting chemistry of the Mn cluster, implicating a very short distance between the phenolic oxygen on Tyr_Z and the Mn cluster (Gilchrist et al., 1995; Hoganson et al., 1995; Tommos et al., 1995).

Upon oxidation, Tyr_Z releases its proton to form a neutral radical. It is likely that the polar residues close to Tyr_Z, together with D1-His190, could participate in transferring this proton to the lumen. The distance between the phenolic oxygen on Tyr_Z and D1-His190 is approximately 4 Å in the model. This suggests that there is no direct hydrogen bond with D1-His190, although an electrostatic interaction is present (Svensson et al., 1990). This is perhaps corroborated by recent experimental results indicating the absence of a well-ordered hydrogen bond for Tyr_Z^{ox} (Tommos et al., 1995; Tang et al., 1995; Un et al., 1996). D1-His190 may still be involved in a hydrogen bond to the peptide oxygen of D1-Leu297, which is symmetrical with the structurally important proposed hydrogen bond close to Tyr_D (see above).

The important role for D1-His190 on the donor side has been experimentally confirmed by site-directed mutagenesis. When D1-His190 in *C. reinhardtii* is mutated to either phenylalanine or tyrosine, the oxygen evolution is lost. However, the EPR spectrum of Tyr_Z^{ox} in the mutant D1-His190 → Phe is very similar to the wild type spectrum (Roffey et al., 1994b), which suggests that the mutation does not modify the close structural environment of Tyr_Z. Tyr_Z is not affected by mutation of D1-His190 to glutamine in *Synechocystis* 6803 as determined from ^2H_2O exchange FTIR spectroscopy (Bernard et al., 1995). Thus, D1-His190 is not in as close contact with Tyr_Z as the corresponding D2-His190 is with Tyr_D. This result is in agreement with the predictions from the structural model, where a longer distance between Tyr_Z and D1-His190 is seen. The Tyr_Z^{ox} radical was also difficult to induce in these mutants, which is probably related to the findings that exchange of D1-His190 to glutamate or aspartate in *Synechocystis* 6803 slowed down the electron transfer from Tyr_Z to P_{680}^+ about 200 times (Diner et al., 1991a; Nixon & Diner, 1994). Similar arguments have also been obtained from fluorescence experiments in mutants in D1-His190 in *C. reinhardtii* (Kramer et al., 1994; Roffey et al., 1994a). D1-His190's importance in electron transfer is perhaps also supported by the observed pK_a of 6−7 in the reduction of P_{680}^+ (Conjeaud & Mathis, 1986), which was proposed to be due to the interaction between the tyrosine and a nearby histidine residue. These results concerning D1-His190 can be explained by a direct involvement of this residue in the electron transfer from Tyr_Z to P_{680} or that it functions as a base accepting the proton from Tyr_Z, thereby facilitating the oxidation of Tyr_Z. Both functions might apply if we consider a concerted electron−proton (hydrogen atom) transfer from Tyr_Z.

Tyr_Z is in the model in van der Waals contact with D1-Phe186, D1-Gln165, and D1-Ala294 on the D1 protein. D1-Phe186 is placed between Tyr_Z and P_{680} and is also likely to be a part of the electron transfer pathway (Figure 4F). This phenylalanine is conserved in the D1 protein. In contrast, the corresponding residue is not conserved in the D2 protein (Figure 1). This might be reasonable since there occurs no fast electron transfer from Tyr_D to P_{680}.

An closer understanding of the function of Tyr_Z is presently evolving, and here the model is useful for structural interpretation of functional hypotheses. There still exist many unresolved questions concerning Tyr_Z, for example, the interaction between Tyr_Z and the presumed Mn binding site and the location of the Mn cluster. Furthermore, which residues are involved in the release of the proton upon oxidation of Tyr_Z and the preferred electron transfer pathway (if any) to P_{680}^+ are yet to be elucidated.

(IV) Comparisons with the Existing Model for PSII. We have compared our model with the previously published model for the PSII reaction center (Ruffle et al., 1993). The backbone structures are similar with a coordinate RMS deviation of 2.08 Å. In contrast, some side-chain and cofactor geometries differ significantly. The coordinate RMS deviations are in the range of up to 8 Å for some residues close to helical ends. However, this is not unexpected since the models are built on protein segments of different lengths.

Smaller, but more significant, are the coordinate RMS deviations of up to 4−5 Å around the two chlorophylls constituting P_{680} and also in the environment of Tyr_Z. We have analyzed these in some detail.

The cofactor geometry in the model of Ruffle et al. (1992) resembles that of the purple bacterium *Rb. sphaeroides* (Allen et al., 1987a). In contrast, our model differs significantly from the purple bacterial reaction center for the chlorophylls constituting the pair, due to our structural optimization of the pigment conformations to fit the available spectra of P_{680}. From our excitonic interaction calculations on several structural arrangements of the chlorophylls in the PSII model, we can conclude that a conformation that resembles the purple bacterial conformation, *i.e.*, with a parallel dimer of chlorophylls approximately 7−8 Å apart, is not in agreement with the excitonic coupling determined from the available spectra of P_{680}. Thus, it seems that, in this region, the structure proposed by Ruffle et al. (1993) does not find support in the existing experimental data. Moreover, in the modeling by Ruffle et al. (1993) no energy calculations were performed on the porphyrin pigments and protein−pigment interactions, which consequently have led to several unfavorable van der Waals contacts not present in our structure.

The structural region around Tyr_Z is also considerably different between our PSII model and the model by Ruffle et al. (1993). The angle between the Cγ (C1) to Cζ (C4, phenol group) axis and the membrane plane is 70° in our model while it is 24° in the model by Ruffle et al. This means that in the model by Ruffle et al. the tyrosyl side chain is turned more toward the inner part of the protein. We can also consider the orientation of Tyr_Z with respect to the symmetrically located Tyr_D on the D2 protein, which in both models is oriented with an angle of approximately 70° with the membrane plane. More important are the orientation studies showing that Tyr_D and Tyr_Z are similarly oriented close to perpendicular to the membrane plane (Mino & Kawamori, 1994), suggesting that the orientation of Tyr_Z is wrong in the model by Ruffle et al.

The part of the acceptor side we have included in our model, the region around the pheophytin and the Fe^{2+}, is very similar to the model by Ruffle et al. In the model by Ruffle et al. the regions of the quinones are included. We have not studied those, but the herbicide binding in the Q_B site of that model has been studied and agrees well with experimental data (Mackay & O'Malley, 1993a,b).

CONCLUSIONS

The present model was obtained by combining assumptions about the structural homology of PSII and the bacterial reaction centers with energetic and spectroscopic considerations. The homology-based modeling approach allowed the coarse structure of the PSII model to be built, *i.e.*, the backbone orientation and the position of identical side-chain atoms. The method we have applied for the energy-based side-chain positioning has been tested earlier on known protein structures: it successfully positioned 92% of the χ_1 and 81% of the χ_2 side-chain dihedral angles of the C-terminal lobe of rhizopuspepsin using as the template the homologous lobe of penicillopepsin. In this case the two proteins had 39% sequence identity (Summers & Karplus, 1989). Most errors were in solvent-exposed side chains while the predictions in the core of the protein were highly accurate. In the present work on the PS II reaction center it is impossible to quantitatively evaluate the errors that will be present. However, as all the residues of interest in the present study are buried, the known uncertainties involved in modeling solvent-exposed side chains are avoided, suggesting that our precision could be high.

The sequence identity between the modeled proteins and the template in the present model is only 22%. This is significantly less than in the rhizopuspepsin test case. However, the similarity (residues with similar size, charge, hydrophobicity, or aromaticity) between the bacterial proteins (L and M subunits in *Rps. viridis*) and the D1 and D2 proteins in PSII in the central region of the model is 50−60%. Furthermore, as described in Results and Discussion, extensive checks of the present model have been made by comparing predictions from the model with the existing body of experimental data on PSII, much of which was derived by a combination of site-directed mutagenesis and spectroscopy to give information on local structural elements in the PSII reaction center.

The model is consistent with the experimental data available at present. The results indicate that the model can serve both as a basis for more advanced structural modeling and computational approaches concerning the PSII reaction center and as an aid in the design of detailed experiments to advance our functional knowledge. For the two redox-active tyrosines the model and the experimental work are in accord. In fact, the model has served as the intellectual basis for several of the experiments done recently with site-directed mutagenesis and EPR spectroscopy on the structures around the tyrosyl radicals. Consequently, this region is perhaps the structurally best characterized in the PSII reaction center. The model also accommodates results from site-directed mutagenesis in the D1 protein around the pheophytin electron acceptor and in the D2 protein around the acceptor-side Fe^{2+}.

To develop a testable proposal for the very important and much debated structural issue around the primary electron donor P_{680}, we have used a new approach to predict the chlorophyll structure. We have applied exciton calculations on P_{680} and compared then with optical spectra in the literature (Svensson et al., 1995). Many configurations of two or more chlorophylls can give rise to the observed optical spectra. However, by using the limited flexibility around P_{680} in the model, we have been able to chose one of these solutions that fit both the optical spectra and the constraints put from the structural model. In this model of the P_{680} dimer, we have accommodated two chlorophyll *a* molecules in a weakly coupled dimer. The predicted center to center distance of the chlorophylls in P_{680} is 10.1 Å, which is larger than the corresponding distance of 7.3 Å in the *Rps. viridis* structure. The two chlorophylls are parallel and the distance between their ring planes is 3.4 Å. The larger separation between the chlorophylls in the dimer produces a more evenly distributed exciton interaction between *all* the pigments in PSII, which corroborates a proposal that a multimer of pigments constitutes P_{680} (Durrant et al., 1995). Furthermore, in our preferred conformation for the chlorophyll pair in P_{680} we have observed two, possibly three, hydrogen bonds between the chlorophylls and residues on the D1 and D2 proteins.

ACKNOWLEDGMENT

We are grateful for valuable contributions and discussions about modeling procedures with Nicolas Foloppe, SBPM, DBCM, CE-Saclay, France.

REFERENCES

Allen, J. P., Feher, G., Yeates, T. O., Komiya, H., & Rees, D. C. (1987a) *Proc. Natl. Acad. Sci. U.S.A. 84*, 5730−5734.

Allen, J. P., Feher, G., Yeates, T. O., Komiya, H., & Rees, D. C. (1987b) *Proc. Natl. Acad. Sci. U.S.A. 84*, 6162−6166.

Andersson, B., & Styring, S. (1991) in *Current Topics in Bioenergetics* (Lee, C. P., Ed.) Vol. 16, pp 1−81, Academic Press Inc., San Diego, CA.

Babcock, G. T., & Sauer, K. (1973) *Biochim. Biophys. Acta 325*, 483−503.

Barber, J. (1993) *Biochem. Soc. Trans. 21*, 981−986.

Becker, M., Middendorf, D., Woodbury, N. W., Parson, W. W., & Blankenship, R. C. (1986) in *Ultrafast Phenomena V* (Fleming, G. R., & Siegman, A. E., Eds.) pp 374−378, Springer, New York.

Bernard, M. T., MacDonald, G. M., Nguyen, A. P., Debus, R. J., & Barry, B. A. (1995) *J. Biol. Chem. 270*, 1589−1594.

Bernstein, F. C., Koetzle, T. F., Williams, G. J. B., Mayer, E. F., Jr., Brice, M. D., Rodgers, J. R., Kennard, O., Shimanouchi, T., & Tasumi, M. (1977) *J. Mol. Biol. 112*, 535−542.

Bock, C. H., Gerken, S., Stehlik, D., & Witt, H. T. (1988) *FEBS Lett. 227*, 141−146.

Bosch, M. K., Evelo, R. G., Styring, S., Rutherford, A. W., & Hoff, A. J. (1991) *FEBS Lett. 292*, 279−283.

Bowyer, J., Hilton, M., Whitelegge, J., Jewess, P., Camilleri, P., Crofts, A., & Robinson, H. (1990) *Z. Naturforsch. 45C*, 379−387.

Braun, P., Greenberg, B. M., & Scherz, A. (1990) *Biochemistry 29*, 10376−10387.

Brooks, B. R., Bruccoleri, R. E., Olafson, B. D., States, D. J., Swaminathan, S. & Karplus, M. (1983) *J. Comput. Chem. 4*, 187−217.

Brown, I. D. (1976) *Acta Crystallogr. A32*, 24−31.

Bunker, G., Stern, E. A., Blankenship, R. E., & Parson, W. W. (1982) *Biophys. J. 37*, 539−551.

Bylina, E. J., Kirmaier, C., McDowell, L., Holten, D., & Youvan, D. C. (1988) *Nature 336*, 182−184.

Carbonera, D., Giacometti, G., & Agostini, G. (1994) *FEBS Lett. 343*, 200−204.

Chang, H. C., Jankowiak, R., Reddy, N. R. S., Yokum, C. F., Picorel, R., Seibert, M., & Small, G. J. (1994) *J. Phys. Chem. 98*, 7725−7735.

Chirino, A. J., Lous, E. J., Huber, M., Allen, J. P., Schenck, C. C., Paddock, M. L., Feher, G., & Rees, D. C. (1994) *Biochemistry 33*, 4584−4593.

Chou, P. Y., & Fasman, G. D. (1974) *Biochemistry 13*, 211−222.

Chow, H.-C., Serlin, R., & Strouse, C. (1975) *J. Am. Chem. Soc. 97*, 7230−7237.

Chu, H.-A., Nguyen, A. P., & Debus, R. J. (1995) *Biochemistry 34*, 5839−5858.

Clarke, A. K., Soitamo, A., Gustavsson, P., & Öquist, G. (1993a) *Proc. Natl. Acad. Sci. U.S.A. 90*, 9973−9977.

Clarke, A. K., Hurry, V. M., Gustavsson, P., & Öquist, G. (1993b) *Proc. Natl. Acad. Sci. U.S.A. 90*, 11985−11989.

Coleman, W. J., & Youvan, D. C. (1990) *Annu. Rev. Biophys. Biophys. Chem. 19*, 333−367.

Conjeaud, H., & Mathis, P. (1986) *Biophys. J. 49*, 1215−1221.

Cowan, S. W., Schirmer, T., Rummel, G., Steier, M., Ghosh, R., Pauptit, R. A., Jansonius, J. N., & Rosenbusch, J. P. (1992) *Nature 358*, 727−733.

Crofts, A., Robinson, H. H., Andrews, K., Van Doren, S., & Berry, E. (1987) in *Cytochrome Systems: Molecular Biology and Bioenergetics* (Papa, S., Chance, B., & Ernster, L., Eds.) pp 617−624, Plenum Publications, New York.

Debus, R. J. (1992) *Biochim. Biophys. Acta 1102*, 269−352.

Debus, R. J., Barry, B. A., Sithole, I., Babcock, G. T., & McIntosh, L. (1988a) *Biochemistry 27*, 9071−9074.

Debus, R. J., Barry, B. A., Babcock, G. T., & McIntosh, L. (1988b) *Proc. Natl. Acad. Sci. U.S.A. 85*, 427−430.

Deisenhofer, J., & Michel, H. (1989) *Science 245*, 1463−1473.

Deisenhofer, J., Epp, O., Miki, K., Huber, R., & Michel, H. (1985) *Nature 318*, 618−624.

De Vitry, C., & Diner, B. (1984) *FEBS Lett. 167*, 327−331.

Dewar, M. J. S., Zoebisch, E. G., Healy, E. F., & Stewart, J. J. P. (1985) *J. Am. Chem. Soc. 107*, 3902−3909.

Diner, B. A., & Petrouleas, V. (1987) *Biochim. Biophys. Acta 895*, 107−125.

Diner, B. A., & Babcock, G. T. (1996) in *Oxygenic Photosynthesis: The Light Reactions* (Ort, D., & Yocum, C. F., Eds.) Kluwer Academic Publishers, Dordrecht, The Netherlands (in press).

Diner, B. A., Nixon, P. J., & Farchaus, J. W. (1991a) *Curr. Opin. Struct. Biol. 1*, 546−554.

Diner, B. A., Petrouleas, V., & Wendoloski, J. J. (1991b) *Physiol. Plant. 81*, 423−436.

Durrant, J. R., Klug, D. R., Kwa, S. L. S., Van Grondelle, R., Porter, G., & Dekker, J. P. (1995) *Proc. Natl. Acad. Sci. U.S.A. 92*, 4798−4802.

Egner, U., Hover, G.-A., & Saenger, W. (1993) *Biochim. Biophys. Acta 1142*, 106−114.

Eijckelhoff, C., & Dekker, J. P. (1995) *Biochim. Biophys. Acta 1231*, 21−28.

Ermler, U., Fritzsch, G., Buchanan, S. K., & Michel, H. (1994) *Structure 2*, 925−936.

Evelo, R. G., Dikanov, S. A., & Hoff, A. J. (1989a) *Chem. Phys. Lett. 157*, 25−30.

Evelo, R. G., Hoff, A. J., Dikanov, S. A., & Tyryshkin, A. M. (1989b) *Chem. Phys. Lett. 161*, 479−484.

Finkele, U., Lauterwasser, C., Zinth, W., Gray, K. A., & Oesterhelt, D. (1990) *Biochemistry 29*, 8517−8521.

Fischer, M. S., Templeton, D. H., Zalkin, A., & Calvin, M. (1972) *J. Am. Chem. Soc. 94*, 3613−3619.

Foloppe, N., Breton, J., & Smith, J. C. (1992) in *The Photosynthetic Bacteria* (Breton, J., & Verméglio, A., Eds.) pp 43−48, Plenum Press, New York.

Foloppe, N., Ferrand, M., Breton, J., & Smith, J. C. (1995) *Proteins 22*, 226−244.

Ghanotakis, D. F., de Paula, J. C., Demetriou, D. M., Bowlby, N. R., Petersen, J., Babcock, G. T., & Yocum, C. F. (1989) *Biochim. Biophys. Acta 974*, 44−53.

Gilchrist, M. L., Jr., Ball, J. A., Randall, D. W., & Britt, R. D. (1995) *Proc. Natl. Acad. Sci. U.S.A. 92*, 9545−9549.

Giorgi, L. B., Nixon, P. J., Merry, S. A. P., Joseph, D. M., Durrant, J. R., De Las Rivas, J., Barber, J., Porter, G., & Klug, D. R. (1996) *J. Biol. Chem. 271*, 2093−2101.

Govindjee (1993) *Z. Naturforsch. 48C*, 251−258.

Henderson, R., Baldwin, J. M., Ceska, T. A., Zemlin, F., Beckmann, E., & Downing, K. H. (1990) *J. Mol. Biol. 213*, 899−929.

Hilbert, M., Böhm, G., & Jaenicke, R. (1993) *Proteins 17*, 138−151.

Hillmann, B., Brettel, K., Van Mieghem, F., Kamlowski, A., Rutherford, A. W., & Schlodder, E. (1995) *Biochemistry 34*, 4814−4827.

Hirsch, D. J., & Brudvig, G. W. (1993) *J. Phys. Chem. 97*, 13216−13222.

Hoganson, C. W., & Babcock, G. T. (1988) *Biochemistry 27*, 5848−5855.

Hoganson, C. W., Lydakis-Simantiris, N., Tang, X.-S., Tommos, C., Warncke, K., Babcock, G. T., Diner, B. A., McCracken, J., & Styring, S. (1995) *Photosynth. Res. 46*, 177−184.

IUPAC−IUB, Joint Comission on Biochemical Nomenclature, Moss, G. B., Ed. (1987) *Pure Appl. Chem. 59*, 779−832.

Kabsch, W., & Sander, C. (1983) *Biopolymers 22*, 2577−2637.

Kirmaier, C., Gaul, D., DeBey, R., Holten, D., & Schenck, C. C. (1991) *Science 251*, 922−927.

Kodera, Y., Takura, K., & Kawamori, A. (1992) *Biochim. Biophys. Acta 1101*, 23−32.

Koulougliotis, D., Tang, X.-S., Diner, B. A., & Brudvig, G. W. (1995) *Biochemistry 34*, 2850-2856.

Kramer, D. M., Roffey, R. A., Govindjee, & Sayre, R. T. (1994) *Biochim. Biophys. Acta 1185*, 228−237.

Kratky, C., & Dunitz, J. D. (1975) *Acta Crystallogr. 31*, 1586−1589.

Kratky, C., & Dunitz, J. D. (1977) *Acta Crystallogr. 33*, 545−547.
Kraulis, P. J. (1991) *J. Appl. Crystallogr. 24*, 946−950.
Kuczera, K., Kuriyan, J., & Karplus, M. (1990) *J. Mol. Biol. 213*, 351−373.
Kühlbrandt, W., Wang, D. N., & Fujiyoshi, Y. (1994) *Nature 367*, 614−621.
Kuhn, M., Fromme, P., & Krabben, L. (1994) *Trends Biochem. Sci. 19*, 401−402.
Kulkarni, R. D., & Golden, S. S. (1994) *J. Bacteriol. 176*, 959−965.
Kwa, S. L. S., Newell, W. R., Van Grondelle, R., & Dekker, J. P. (1992) *Biochim. Biophys. Acta 1099*, 193−202.
Kwa, S. L. S., Eijckelhoff, C., Van Grondelle, R., & Dekker, J. P. (1994) *J. Phys. Chem. 98*, 7702−7711.
Langen, R., Brayer, G. D., Berghuis, A. M., McLendon, G., Sherman, F., & Warshel, A. (1992) *J. Mol. Biol. 224*, 589−600.
Laskowski, R. A., MacArthur, M. W., Moss, D. S., & Thornton, J. M. (1993) *J. Appl. Crystallogr. 26*, 283−291.
Lubitz, W., Isaacson, R. A., Okamura, M. Y., Abresch, E. C., Plato, M., & Feher, G. (1989) *Biochim. Biophys. Acta 977*, 227−232.
MacArthur, M. W., & Thornton, J. M. (1991) *J. Mol. Biol. 218*, 397−412.
Mackay, S. P., & O'Malley, P. J. (1993a) *Z. Naturforsch. 48C*, 773−781.
Mackay, S. P., & O'Malley, P. J. (1993b) *Z. Naturforsch. 48C*, 782−787.
McLachlan, A. D. (1982) *Acta Crystallogr. A38*, 871−873.
Metz, J. G., Nixon, P. J., Rögner, M., Brudvig, G. W., & Diner, B. A. (1989) *Biochemistry 28*, 6960−6969.
Michel, H., & Deisenhofer, J. (1988) *Biochemistry 27*, 1−7.
Michel, H., Weyer, K. A., Gruenberg, H., Dunger, I., Oesterhelt, D., & Lottspeich, F. (1986) *EMBO J. 5*, 1149−1158.
Mino, H., & Kawamori, A. (1994) *Biochim. Biophys. Acta 1185*, 213−220.
Moënne-Loccoz, P., Robert, B., & Lutz, M. (1989) *Biochemistry 28*, 3641−3645.
Mulkidjanian, A. Y., Cherepanov, D. A., Haumann, M., & Junge, W. (1996) *Biochemistry 35*, 3093−3107.
Mulliken, R. S. (1955) *J. Chem. Phys. 23*, 1833−1846.
Nabedryk, E., Andrianambinintsoa, S., Berger, G., Leonhard, M., Mäntele, W., & Breton, J. (1990) *Biochim. Biophys. Acta 1016*, 49−54.
Nanba, O., & Satoh, K. (1987) *Proc. Natl. Acad. Sci. U.S.A. 84*, 109−112.
Nixon, P. J., & Diner, B. A. (1992) *Biochemistry 31*, 942−948.
Nixon, P. J., & Diner, B. A. (1994) *Biochem. Soc. Trans. 22*, 338−343.
Noguchi, T., Inoue, Y., & Satoh, Ki. (1993) *Biochemistry 32*, 7186−7195.
Ohad, N., Keasar, C., & Hirschberg, J. (1992) in *Research in Photosynthesis* (Murata, N., Ed.) Vol. II, pp 223−226, Kluwer Academic Publishers, Dordrecht, The Netherlands.
O'Malley, P. J., Babcock, G. T., & Prince, R. P. (1984) *Biochim. Biophys. Acta 766*, 283−288.
Otsuka, J., Miyachi, H., & Horimoto, K. (1992) *Biochim. Biophys. Acta 1118*, 194−210.
Pakrasi, H. B., & Vermaas, W. F. J. (1992) in *The Photosystems: Structure, Function and Molecular Biology* (Barber, J., Ed.) pp 2331−257, Elsevier Science Publishers, Amsterdam, The Netherlands.
Pearlstein, R. M. (1991) in *Chlorophylls* (Scheer, H., Ed.) pp 1047−1078, CRC Press, Boca Raton, FL.
Petrouleas, V., & Diner, B. A. (1990) *Biochim. Biophys. Acta 1015*, 131−140.
Pfister, K., Steinback, K. E., Gardner, G., & Arntzen, C. J. (1981) *Proc. Natl. Acad. Sci. U.S.A. 78*, 981−985.
Protein Data Bank (1992) *Atomic Coordinate and Bibliographic Entry Format Description*, Brookhaven National Laboratory, Upton, NY.
Ramachandran, G. N., Ramakrishnan, C., & Sasisekharan, V. (1963) *J. Mol. Biol. 7*, 95−99.
Rigby, S. E. J., Nugent, J. H. A., & O'Malley, P. J. (1994) *Biochemistry 33*, 1734−1742.
Rodrigues, I. D., Chandrashekar, T. K., & Babcock, G. T. (1987) in *Progress in Photosynthesis* (Biggins, J., Ed.) Vol. I, pp 119−133, Martinus Nijhoff Publishers, Dordrecht, The Netherlands.
Roffey, R. A., Kramer, D. M., Govindjee, & Sayre, R. T. (1994a) *Biochim. Biophys. Acta 1185*, 257−270.
Roffey, R. A., Van Wijk, K.-J., Sayre, R. T., & Styring, S. (1994b) *J. Biol. Chem. 269*, 5115−5121.
Ruffle, S. V., Donnelly, D., Blundell, T. L., & Nugent, J. H. A. (1992) *Photosynth. Res. 34*, 287−300.
Rutherford, A. W. (1985) *Biochim. Biophys. Acta 807*, 189−201.
Rutherford, A. W. (1987) in *Progress in Photosynthesis Research* (Biggins, J., Ed.) Vol. I, pp 277−283, Martinus Nijhoff Publishers, Dordrecht, The Netherlands.
Rutherford, A. W. (1989) *Trends Biochem. Sci. 14*, 227−232.
Rutherford, A. W., & Zimmermann, J.-L. (1984) *Biochim. Biophys. Acta 767*, 168−175.
Satoh, K. (1993) in *The Photosynthetic Reaction Center* (Deisenhofer, J., & Norris, J. R., Eds.) Vol. I, pp 289−318, Academic Press, San Diego, CA.
Sayre, R. T., Andersson, B., & Bogorad, L. (1986) *Cell 47*, 601−608.
Schelvis, J. P. M., Van Noort, P. I., Aartsma, T. J., & Van Gorkom, H. J. (1994) *Biochim. Biophys. Acta 1184*, 123−131.
Scherer, P. O. J., & Fischer, S. F. (1991) in *Chlorophylls* (Scheer, H., Ed.) pp 1079−1093, CRC Press, Boca Raton, FL.
Seibert, M. (1993) in *The Photosynthetic Reaction Center* (Deisenhofer, J., & Norris, J. R., Eds.) Vol. I, pp 319−356, Academic Press, San Diego, CA.
Smith, J. C., & Karplus, M. (1992) *J. Am. Chem. Soc. 114*, 801−812.
Sobolev, V., & Edelman, M. (1995) *Proteins: Struct., Funct., Genet. 21*, 214−225.
Stilz, H. U., Finkele, U., Holzapfel, W., Lauterwasser, C., Zinth, W., & Oesterhelt, D. (1994) *Eur. J. Biochem. 223*, 233−242.
Stocker, J. W., Tagushi, A. K. W., Murchison, H. A., Woodbury, N. W., & Boxer, S. G. (1992) *Biochemistry 31*, 10536−10362.
Summers, N. L., & Karplus, M. (1989) *J. Mol. Biol. 210*, 785−811.
Summers, N. L., Carlson, W. D., & Karplus, M. (1987) *J. Mol. Biol. 196*, 175−198.
Svensson, B., Vass, I., Cedergren, E., & Styring, S. (1990) *EMBO J. 9*, 2051−2059.
Svensson, B., Vass, I., & Styring, S. (1991) *Z. Naturforsch. 46C*, 765−776.
Svensson, B., Etchebest, C., Tuffery, P., Smith, J., & Styring, S. (1992) in *Research in Photosynthesis* (Murata, N., Ed.) Vol. II, pp 147−150, Kluwer Academic Publishers, Dordrecht, The Netherlands.
Svensson, B., Van Kan, P. J. M., & Styring, S. (1995) in *Photosynthesis: from Light to Biosphere* (Mathis, P., Ed.) Vol. I, pp 425−430, Kluwer Academic Publishers, Dordrecht, The Netherlands.
Takahashi, K., Obayashi, M., & Nishikawa, Y. (1984) *Kin. Daigaku Rik. Kenk. Hokoku 20*, 85−89.
Tang, X.-S., Chisholm, D. A., Dismukes, G. C., Brudvig, G. W., & Diner, B. A. (1993) *Biochemistry 32*, 13742−13748.
Tang, X.-S., Zheng, M., Chisholm, D. A., Dismukes, G. C., & Diner, B. A. (1996) *Biochemistry 35*, 1475−1484.
Telfer, A., De Las Rivas, J., & Barber, J. (1991) *Biochim. Biophys. Acta 1060*, 106−114.
Tietjen, K. G., Kluth, J. F., Andree, R., Haug, M., Lindig, M., Müller, K. H., Wroblonsky, H. J., & Trebst, A. (1991) *Pestic. Sci. 31*, 65−72.
Tommos, C., Davidsson, L., Svensson, B., Madsen, C., Vermaas, W., & Styring, S. (1993) *Biochemistry 32*, 5436−5441.
Tommos, C., Madsen, C., Styring, S., & Vermaas, W. (1994) *Biochemistry 33*, 11805−11813.
Tommos, C., Tang, X.-S., Warncke, K., Hoganson, C. W., Styring, S., McCracken, J., Diner, B. A., & Babcock, G. T. (1995) *J. Am. Chem. Soc. 117*, 10325−10335.
Trebst, A. (1986) *Z. Naturforsch. 41C*, 240−245.
Trebst, A. (1987) *Z. Naturforsch. 42C*, 742−750.
Treutlein, H., Schulten, K., Brünger, A. T., Karplus, M., Deisenhofer, J., & Michel, H. (1992) *Proc. Natl. Acad. Sci. U.S.A. 89*, 75−79.

Tronrud, D. E., Schmid, M. F., & Matthews, B. W. (1986) *J. Mol. Biol. 188*, 443−454.

Tuffery, P., Etchebest, C., Hazout, S., & Lavery, R. (1991) *J. Biomol. Struct. Dyn. 8*, 1267−1289.

Un, S., Brunel, L.-C., Brill, T. M., Zimmermann, J.-L., & Rutherford, A. W. (1994) *Proc. Natl. Acad. Sci. U.S.A. 91*, 5262−5266.

Un, S., Tang, X.-S., & Diner, B. A. (1996) *Biochemistry 35*, 679−684.

Van Gorkom, H. J., & Schelvis, J. P. M. (1993) *Photosynth. Res. 38*, 297−301.

Van Kan, P. J. M., Otte, S. C. M., Kleinherenbrink, F. A. M., Nieveen, M. C., Aartsma, T. J., & Van Gorkom, H. J. (1990) *Biochim. Biophys. Acta 1020*, 146−152.

Van Kan, P. J. M., Groot, M.-L., Kwa, S. L. S., Dekker, J. P., & Van Grondelle, R. (1992) in *The Photosynthetic Bacterial Reaction Center II* (Breton, J., & Verméglio, A., Eds.) pp 411−420, Plenum Press, New York.

Van Mieghem, F. J. E., Satoh, K., & Rutherford, A. W. (1991) *Biochim. Biophys. Acta 1058*, 379−385.

Van Rensen, J. J. S., Tonk, W. J. M., & de Bruijn, S. M. (1988) *FEBS Lett. 226*, 347−351.

Vasha, F., Joseph, D. M., Durrant, J. R., Telfer, A. Klug, D. R., Porter, G., & Barber, J. (1995) *Proc. Natl. Acad. Sci. U.S.A. 92*, 2929−2933.

Vass, I., & Styring, S. (1991) *Biochemistry 30*, 830−839.

Vermaas, W. (1993) *Annu. Rev. Plant Physiol. Plant Mol. Biol. 44*, 457−481.

Vermaas, W. F. J., Rutherford, A. W., & Hansson, Ö. (1988) *Proc. Natl. Acad. Sci. U.S.A. 85*, 8477−8481.

Vermaas, W., Charité, J., & Shen, G. (1990a) *Z. Naturforsch. 45C*, 359−365.

Vermaas, W., Charité, J., & Shen, G. (1990b) *Biochemistry 29*, 5325−5332.

Vermaas, W., Styring, S., Schröder, W. P., & Andersson, B. (1993) *Photosynth. Res. 38*, 249−263.

Vermaas, W., Vass, I., Eggers, B., & Styring, S. (1994) *Biochim. Biophys. Acta 1184*, 263−272.

Vermaas, W. F. J., Williams, J. G. K., & Arntzen, C. J. (1987) *Z. Naturforsch. 42C*, 762−768.

von Heijne, G. (1991) *J. Mol. Biol. 218*, 499−503.

Wachtveitl, J., Farchaus, J. W., Das, R., Lutz, M., Robert, B., & Mattioli, T. (1993) *Biochemistry 32*, 12875−12886.

Warncke, K., Babcock, G. T., & McCracken, J. (1994) *J. Am. Chem. Soc. 116*, 7332−7340.

Weiss, M. S., Abele, U., Weckesser, J., Welte, W., Schiltz, E., & Schultz, G. E. (1991) *Science 254*, 1627−1630.

Williams, J. C., Steiner, L. A., Ogden, R. C., Simon, M. I., & Feher, G. (1983) *Proc. Natl. Acad. Sci. U.S.A. 80*, 6505−6509.

Williams, J. C., Steiner, L. A., Feher, G., & Simon, M. I. (1984) *Proc. Natl. Acad. Sci. U.S.A. 81*, 7303−7307.

Williams, J. C., Alden, R. G., Murchison, H. A., Peloquin, J. M., Woodbury, N. W., & Allen, J. P. (1992) *Biochemistry 31*, 11029−11037.

Wraight, C. (1982) in *Function of Quinones in Energy Conserving Systems* (Trumpower, B. L., Ed.) pp 181−197, Academic Press, New York.

Youvan, D. C., Bylina, E. J., Alberti, M., Begusch, H., & Hearst, J. E. (1984) *Cell 37*, 949−957.

BI960764K